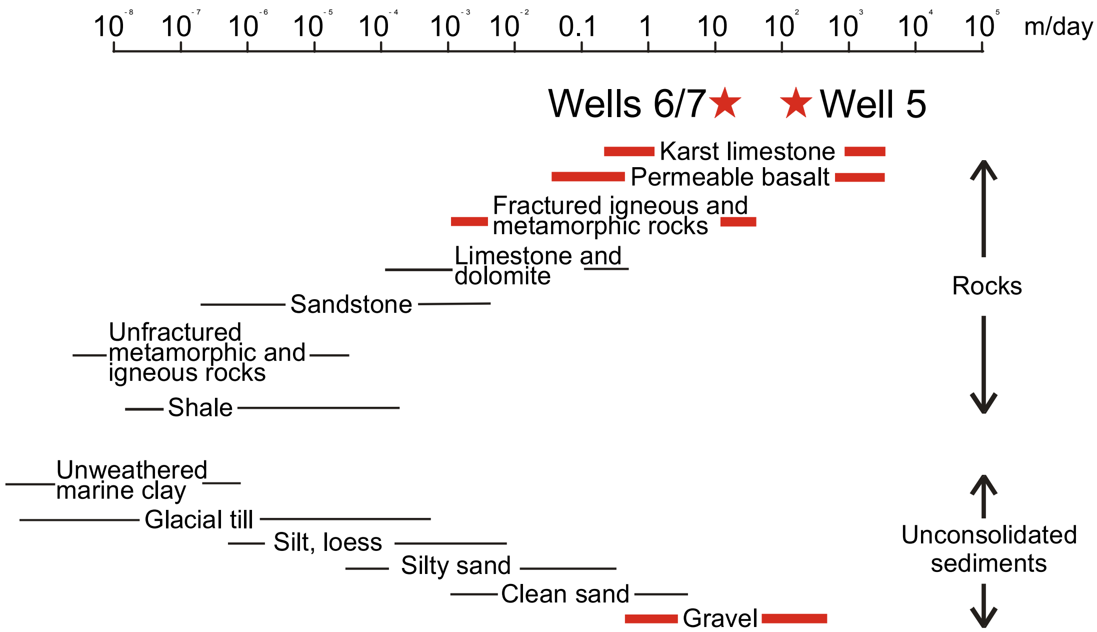

Notes:

1) Velocity in this diagram is calculated from the hydraulic conductivity values of Freeze and Cherry (1979, p. 29, reproduced in Exhibit 261), from the hydraulic gradient at Walkerton (0.002), and from an effective porosity of 35% for unconsolidated materials, 10% for sandstone, and 0.1% for other rocks.

2) Aquifers considered by the US EPA to be susceptible to bacterial contamination are shown with bold bars.

3) Estimated velocities for Walkerton wells using the pumping test results are shown with asterisks.

Figure 1 Comparison of groundwater velocities in rocks and unconsolidated sediments

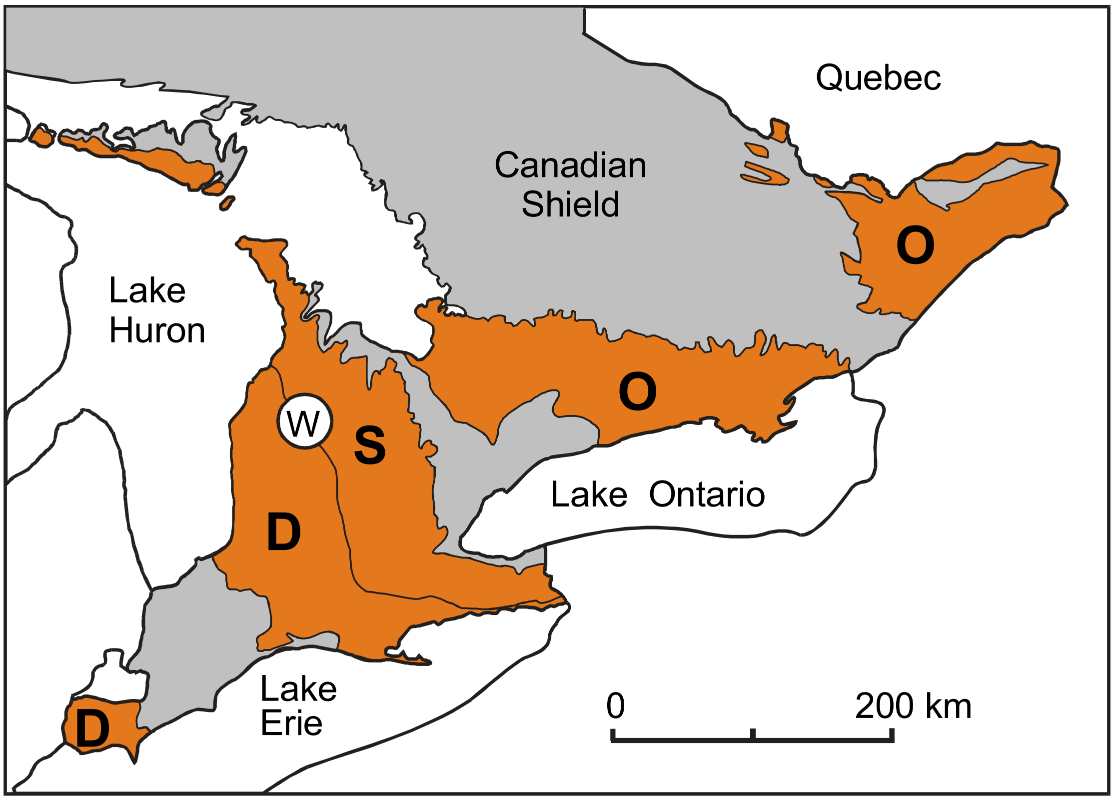

W Walkerton
O Ordovician carbonates
S Silurian carbonates
D Devonian carbonates

Figure 2 Distribution of carbonate bedrock in southern Ontario

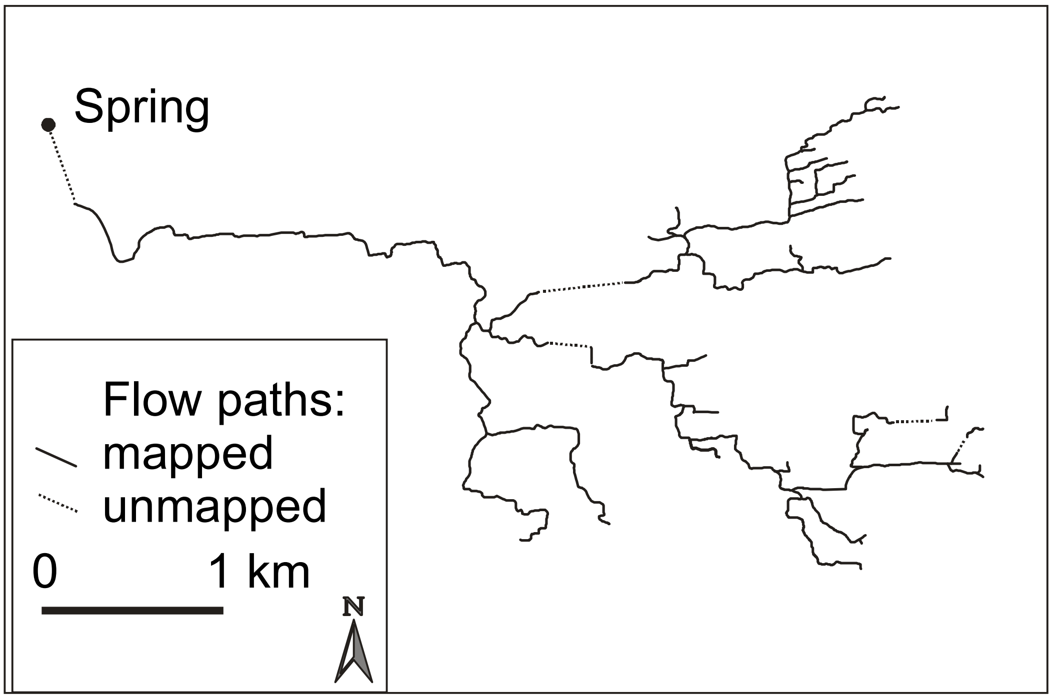

Figure 3 Convergent flow paths draining to a spring, as mapped in Blue Spring Cave, Indiana (after Palmer, 1969)

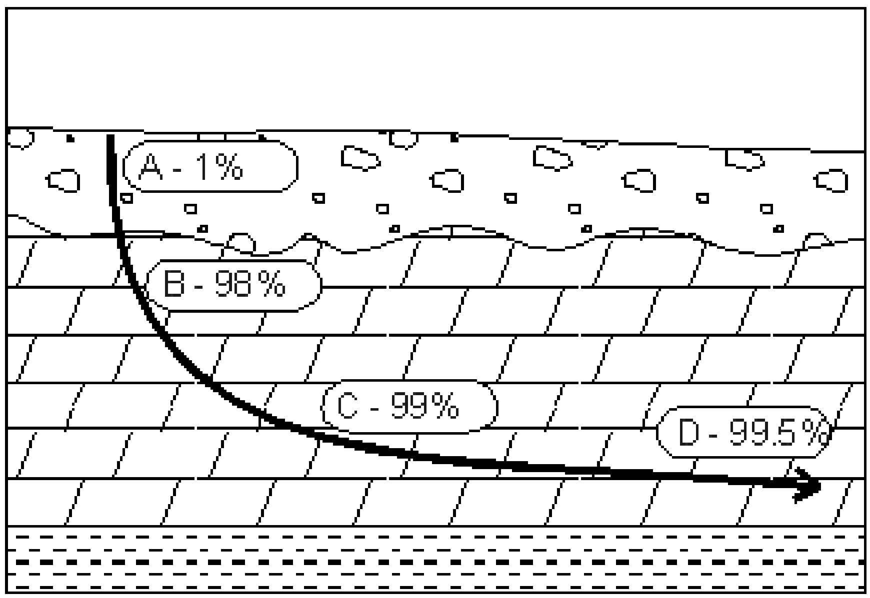

Figure 4 Distribution of solution in carbonate bedrock overlain by overburden. Approximately 2% of solution takes place in the bedrock.

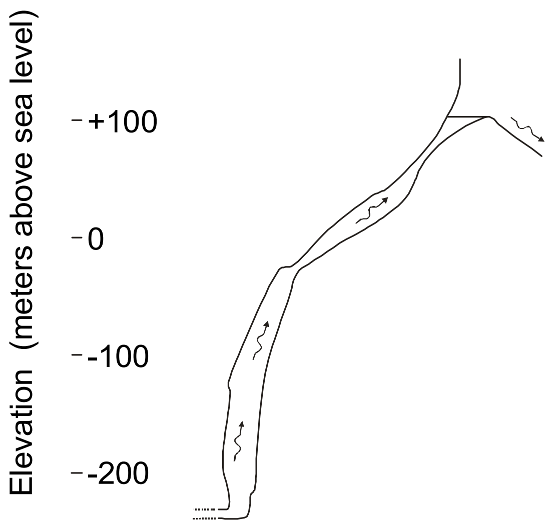

Figure 5 Profile through the Vaucluse Spring in France, explored to a depth of more than 300 m below the water table. A tracer test from 30 km away arrived at the spring in just six days, illustrating that groundwater 300 m below the water table is not necessarily safe from bacterial contamination.

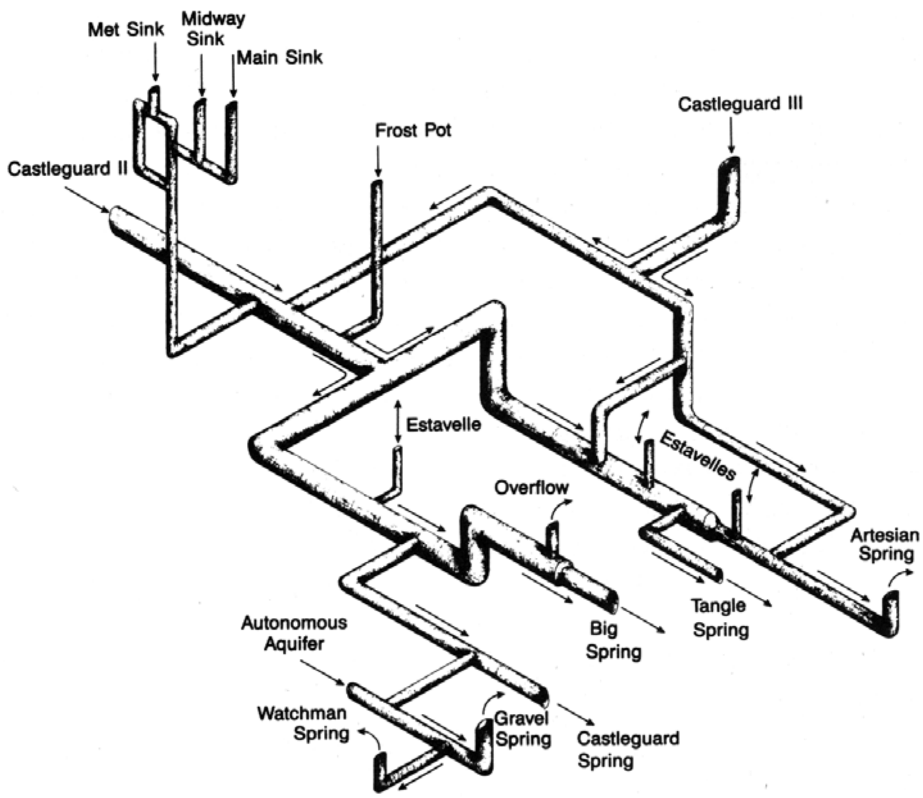

Figure 6.32 Proportional geometric model of Castleguard II conduit system, Canada. From C. Smart (1983b)

Figure 6 Major conduits associated with Castleguard Springs, near Columbia Icefield, Alberta, as deduced from tracer testing, natural discharge pulse analysis, and isotope and chemograph analysis (from Ford and Williams, 1989)

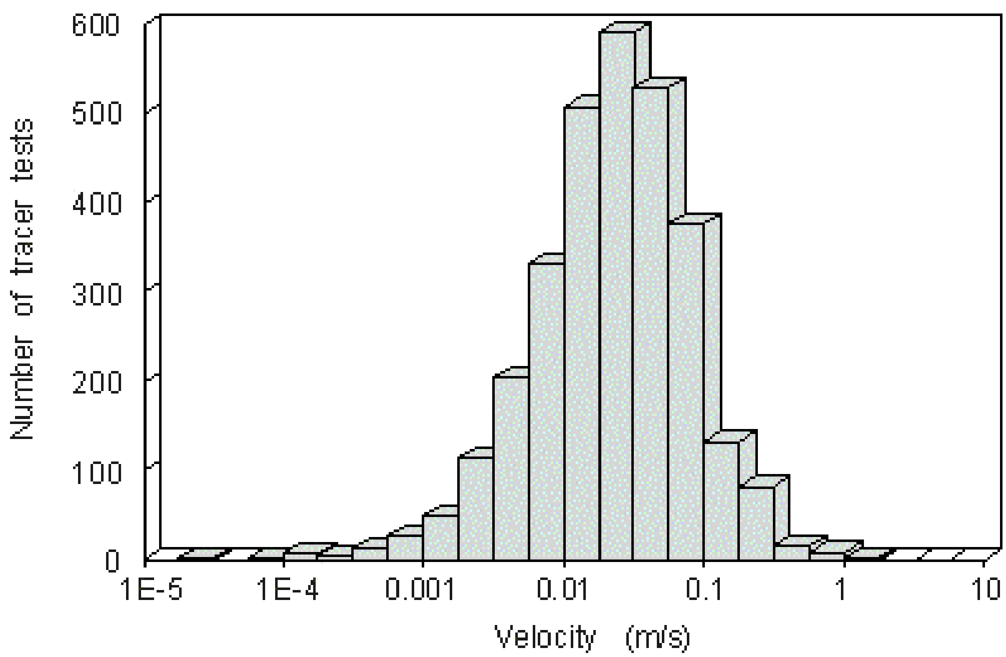

Figure 7 Groundwater flow velocities in conduits in carbonates (from Worthington, Davies, and Ford, 2000; see Exhibit 261)

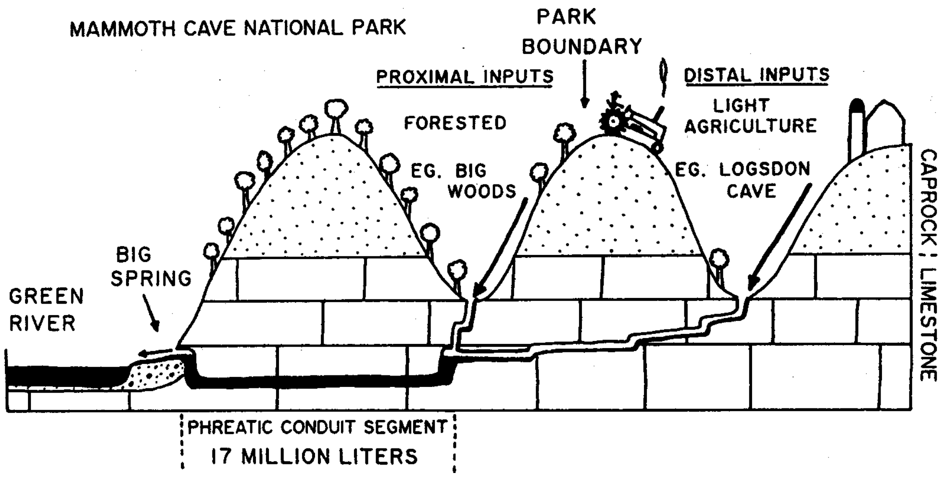

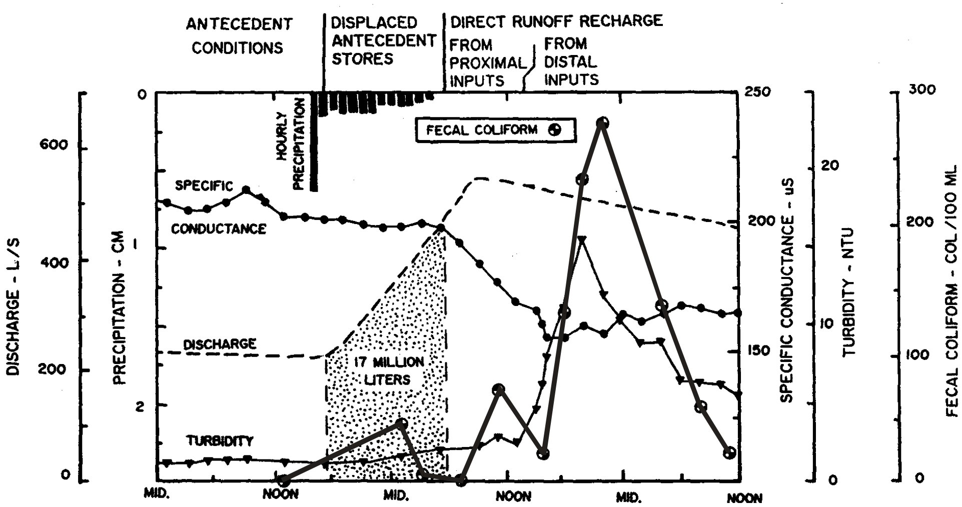

Figure 8 Flow in the karstic drainage flowing to Big Spring, Kentucky. Top: cross-section of the karst system. Bottom: Changes in water quality and discharge over a period of 60 hours (after Ryan and Meiman, 1996; see Appendix 2)

Figure 9 Drainage from the spring close to Well 5. Top: the creek on the south side of the road leading to Well 5. Bottom: the gauging structure at the point where the south creek spring emerges from the culvert and joins the north spring creek. This point is 60 m from Well 5.

Figure 10 Four views of Spring B, midway between Wells 6 and 7, on July 3 2001

Top left 7:50 a.m. Well 7 started pumping at 5:15 a.m. The flow out of the spring is 2.4 L/s (32 gallons per minute)

Top right: 7:50 a.m. The spring emerges from a pipe about 10 m long. The actual location of the spring is at the area of bare soil in the background.

Bottom left: 4:55 p.m. Well 7 has now been pumping continuously for 11 hours and 40 minutes. The water level has now declined to the point where the spring has ceased flowing and 0.22 L/s (2.9 gallons per minute) are flowing from the surface into the aquifer. The plywood weir is acting as a dam, preventing even more inflow into the aquifer.

Bottom right: 4:55 p.m. A vertical view of the water flowing over the weir and into the aquifer.

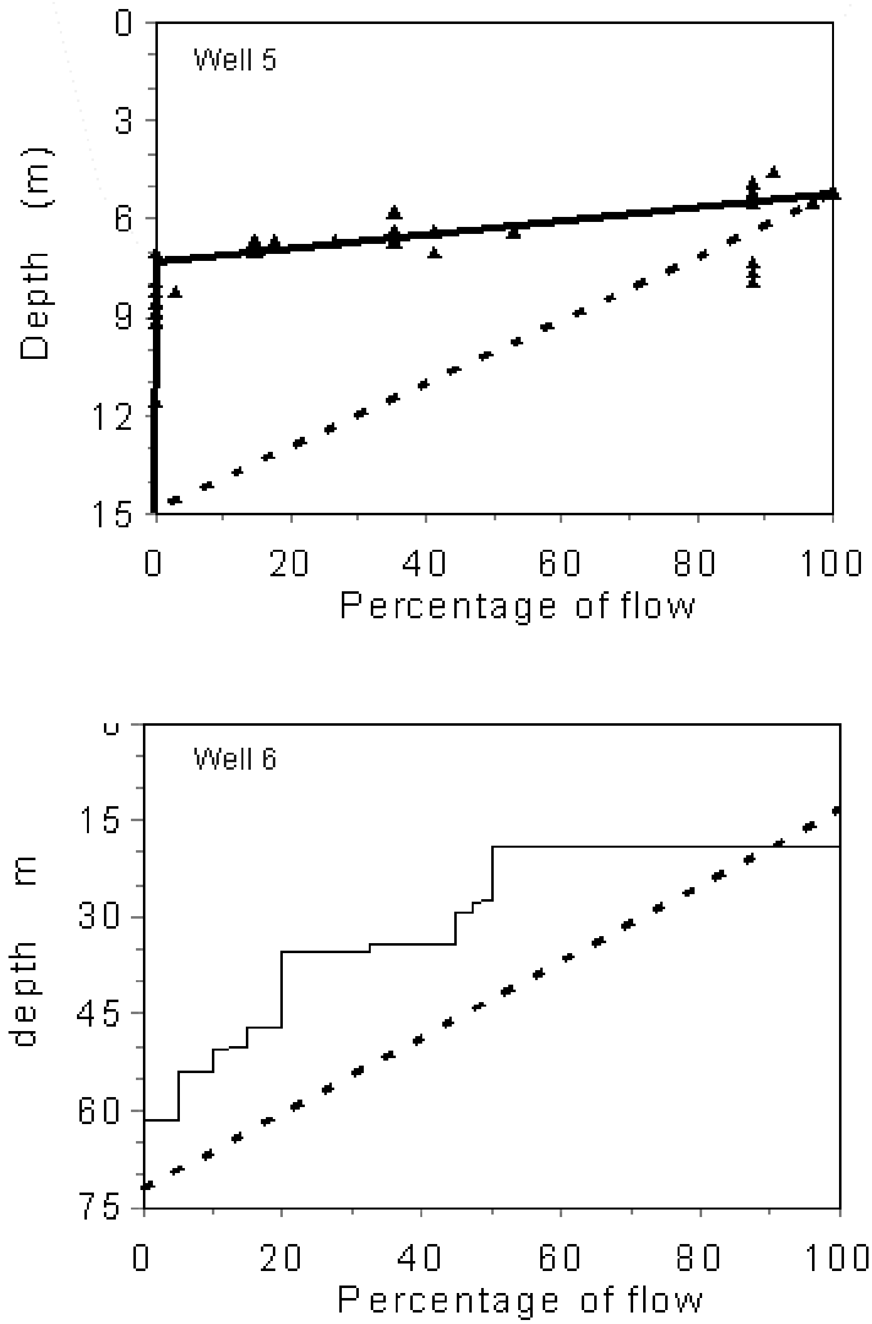

Figure 11 Inflows to Wells 5 (top) and 6 (bottom). The solid lines represent interpretations by Golder Associates for where the inflows occur. The dashed lines indicate a gradual increase in flow which would occur in a porous medium aquifer such as sand (data from Golder Associates, 2000a).

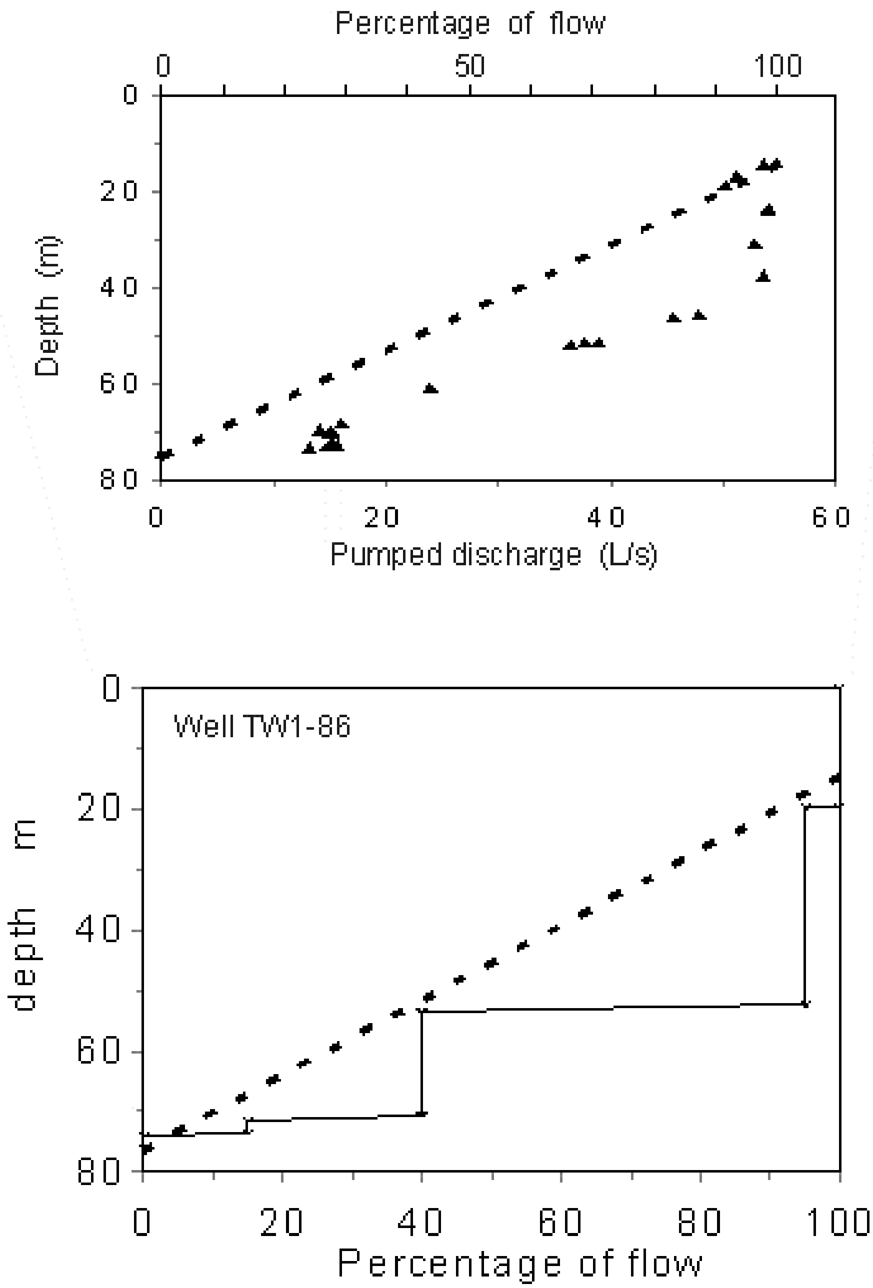

Figure 12 Inflows to Wells 7 (top) and TW1-86 (bottom). The thin solid line represents the interpretation by Golder Associates for where the inflows occur. The dashed lines indicate a gradual increase in flow which would occur in a porous medium aquifer such as sand (data from Golder Associates, 2000a).

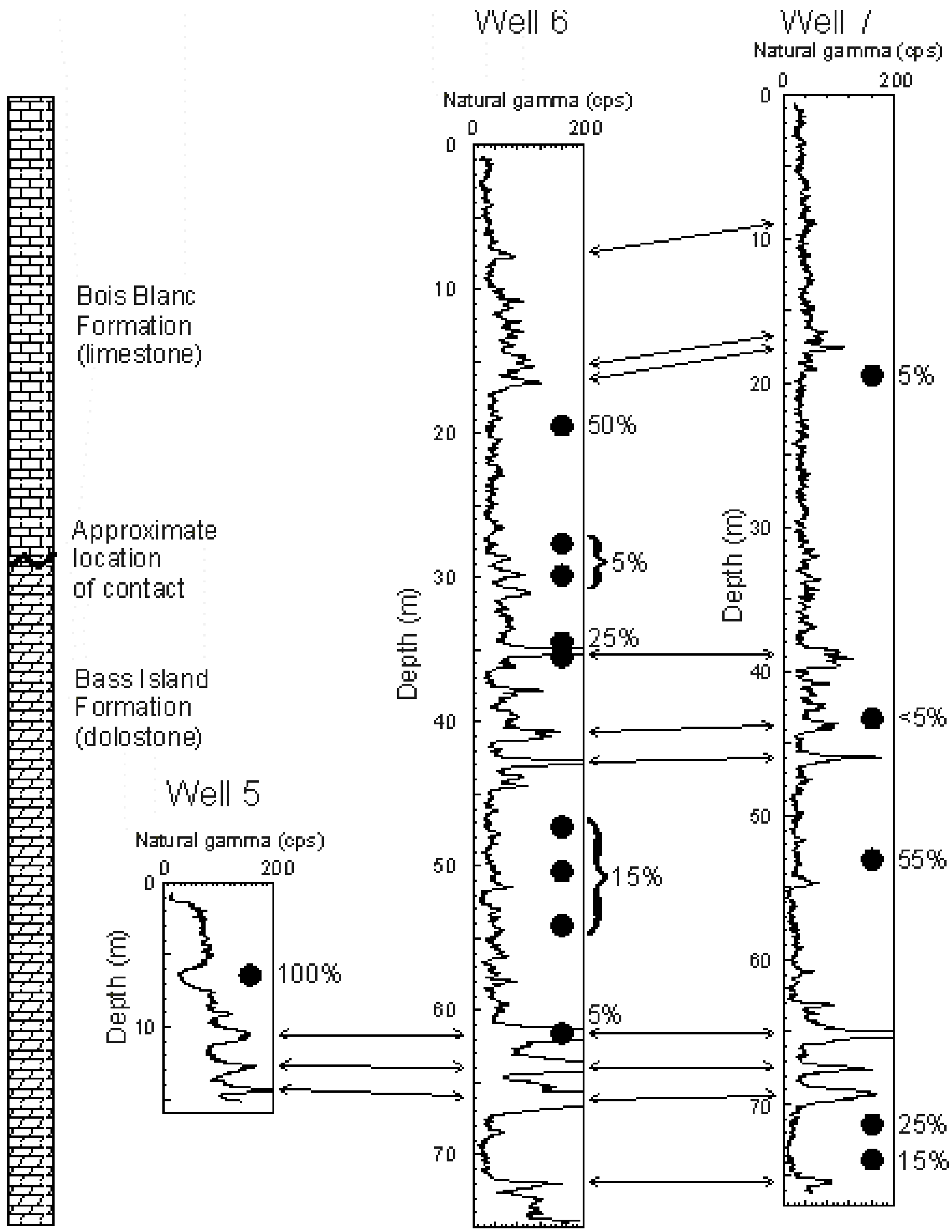

Figure 13 Stratigraphic correlation of Wells 5, 6, and 7 using gamma logs run by Golder Associates, showing the major locations of inflow to the wells. There are no precise locations for inflows to Well 7, so the inflows for the adjacent test well (TW1-86) are substituted. The locations and percentages of inflow to the wells are also shown.

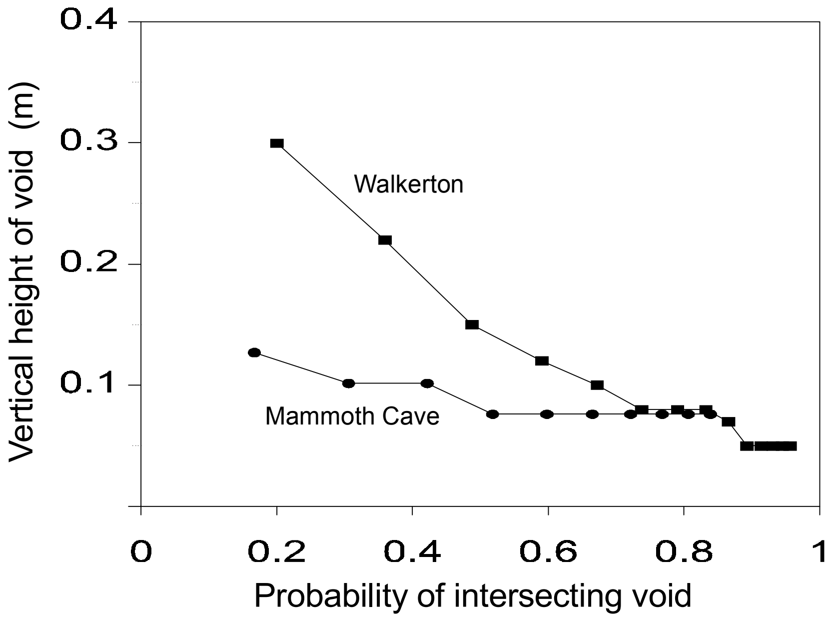

Figure 14 Probabilities per borehole of intersecting a void, showing that larger voids were intersected in five boreholes at Walkerton than in six boreholes in the Mammoth Cave area. The Mammoth Cave boreholes averaged 55 m in depth.

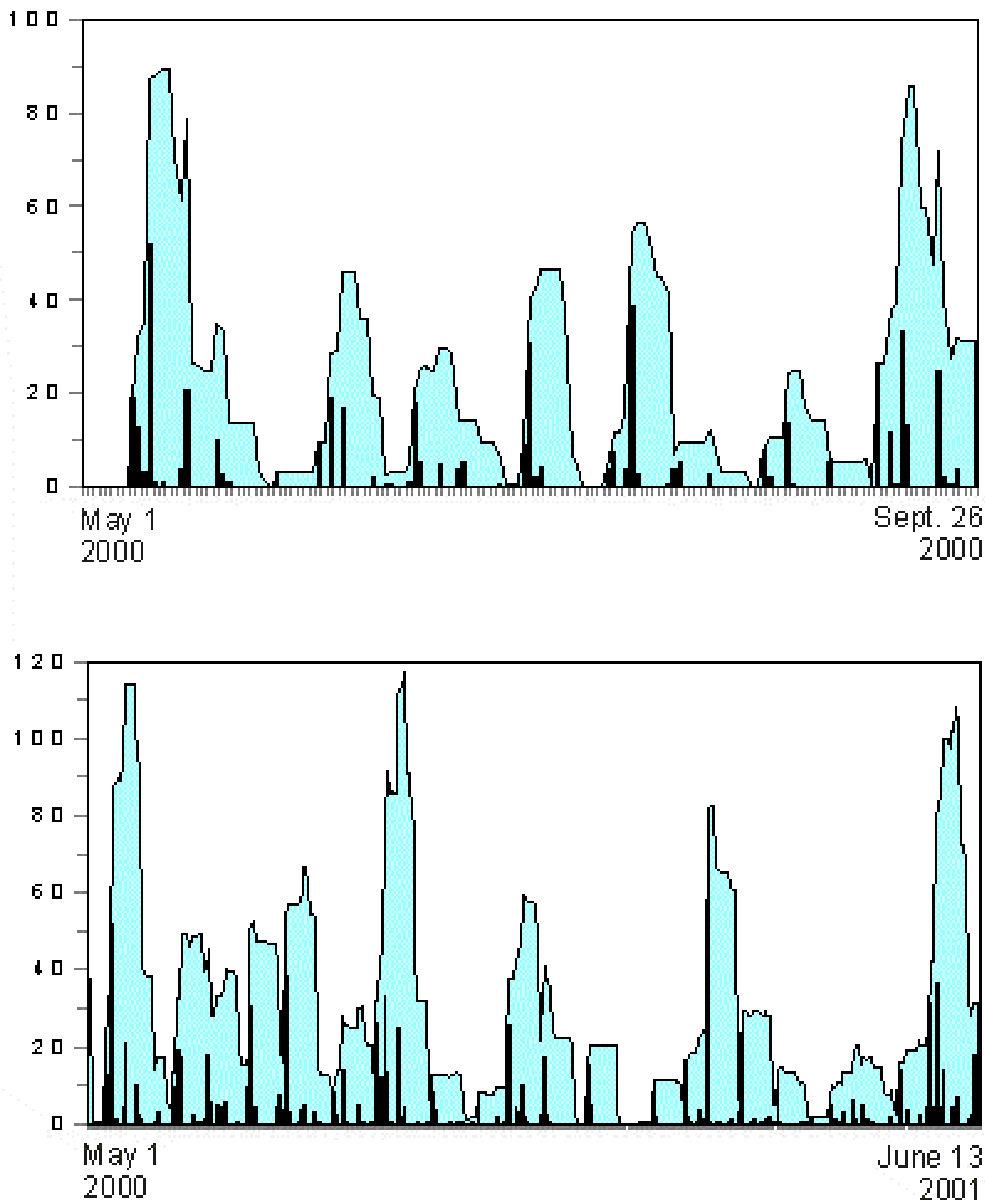

Figure 15 Daily rainfall at Hanover (from Saugeen Valley Conservation Authority gauge) up to April 20 2001 and afterwards at a gauge beside Well 7. The top figure also shows running weekly averages and the bottom figure also shows running two-weekly averages.

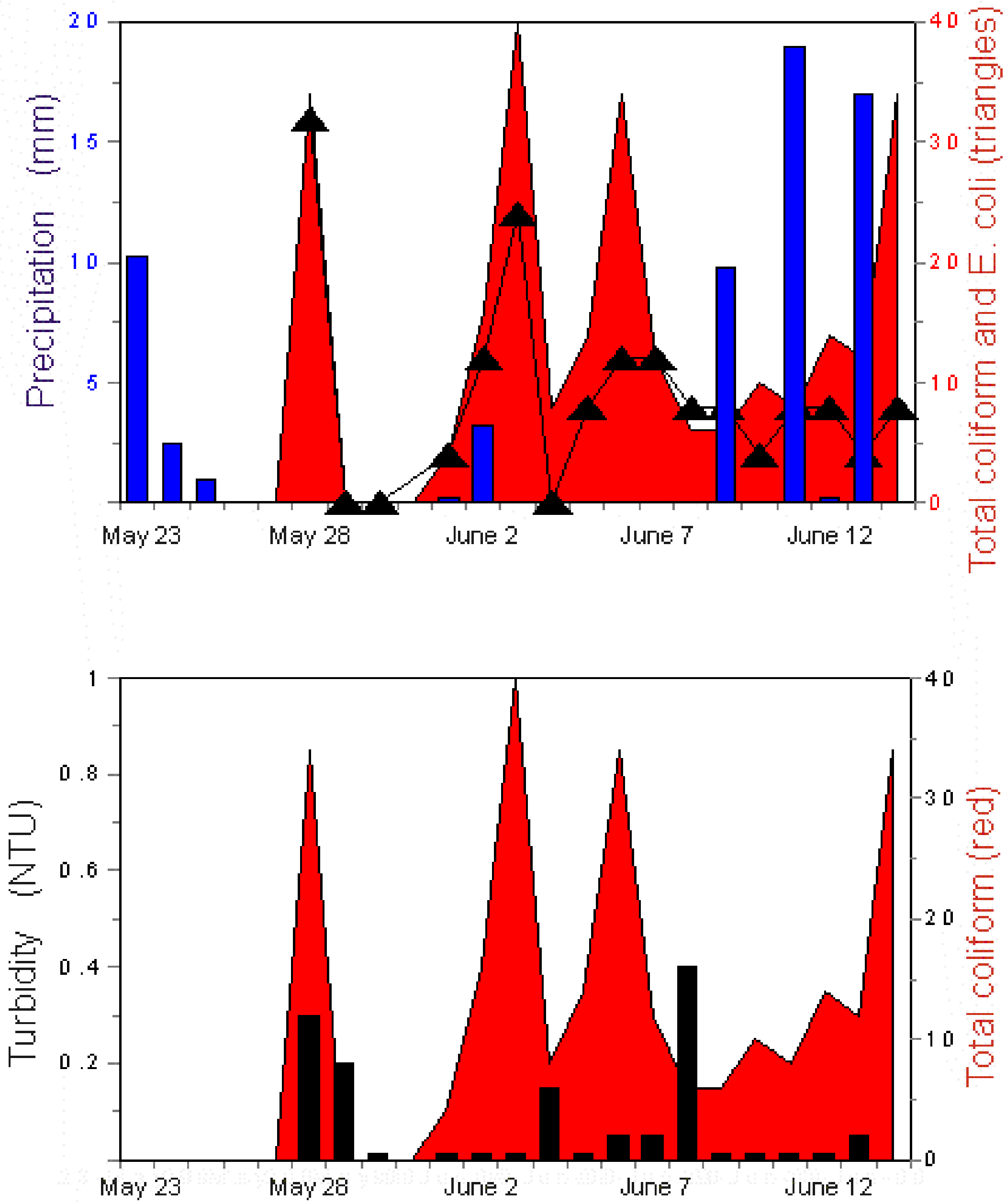

Figure 16 Bacteria data from Well 5 (after OCWA, 2001a). Top: total coliform (solid) and E. Coli (triangles) in Well 5 raw water from May 28 to June 14 2000, compared to precipitation (bars) from May 23 to June 14 2000. Bottom: total coliform (solid) and turbidity (bars) in Well 5 raw water from May 28 to June 14 2000.

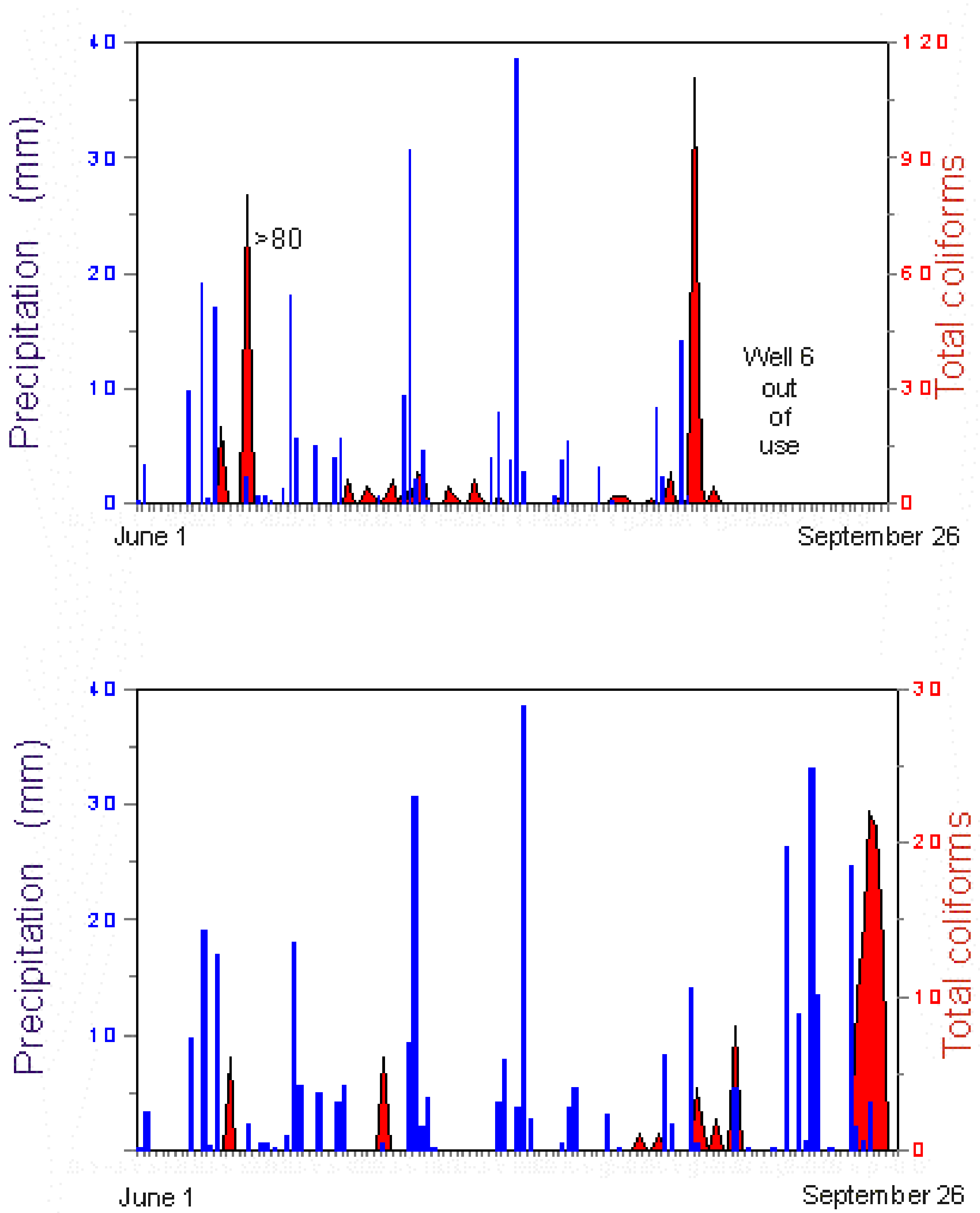

Figure 17 Total coliforms in the raw water (after OCWA, 2001 a,b) at Well 6 (top) and Well 7 (bottom) from June 1 to September 26 2000 together with precipitation at Hanover.

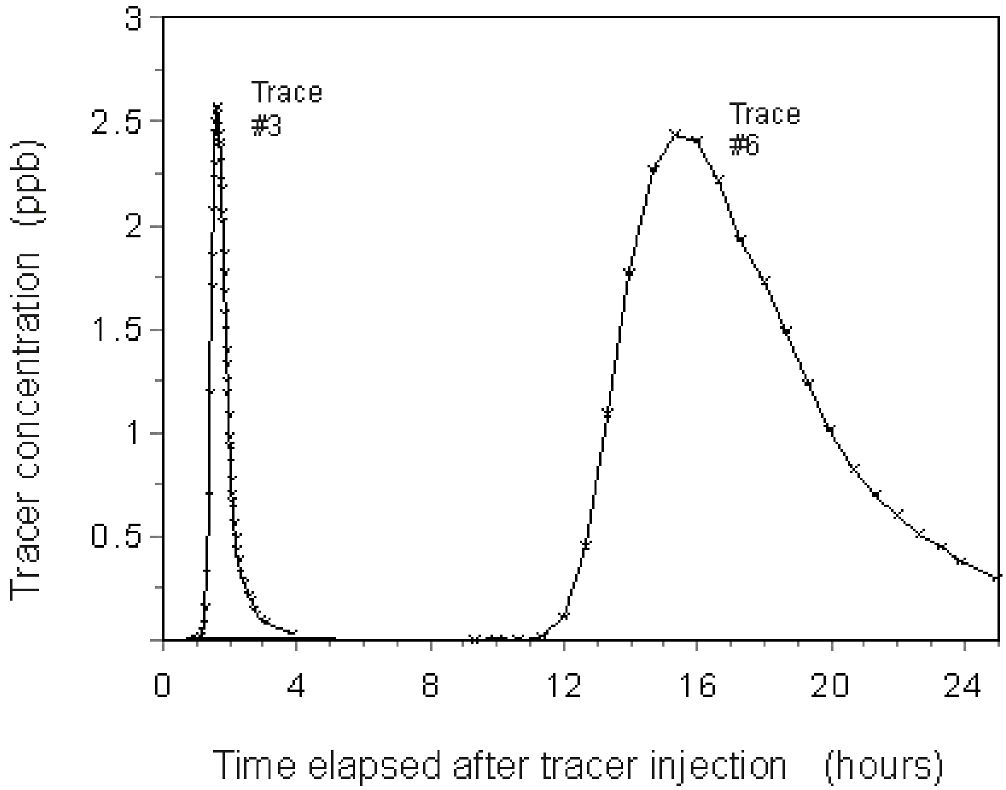

Figure 18 Two groundwater traces from a sinking stream to a spring in Smithville, Ontario. Both traces are along the same flow path, but trace #3 was in high-flow conditions whereas trace #6 was in low-flow conditions. The dye recovery curves are both normalised to a 1 g injection. Modified from Worthington, S.R.H., and D.C.Ford (1997b)..

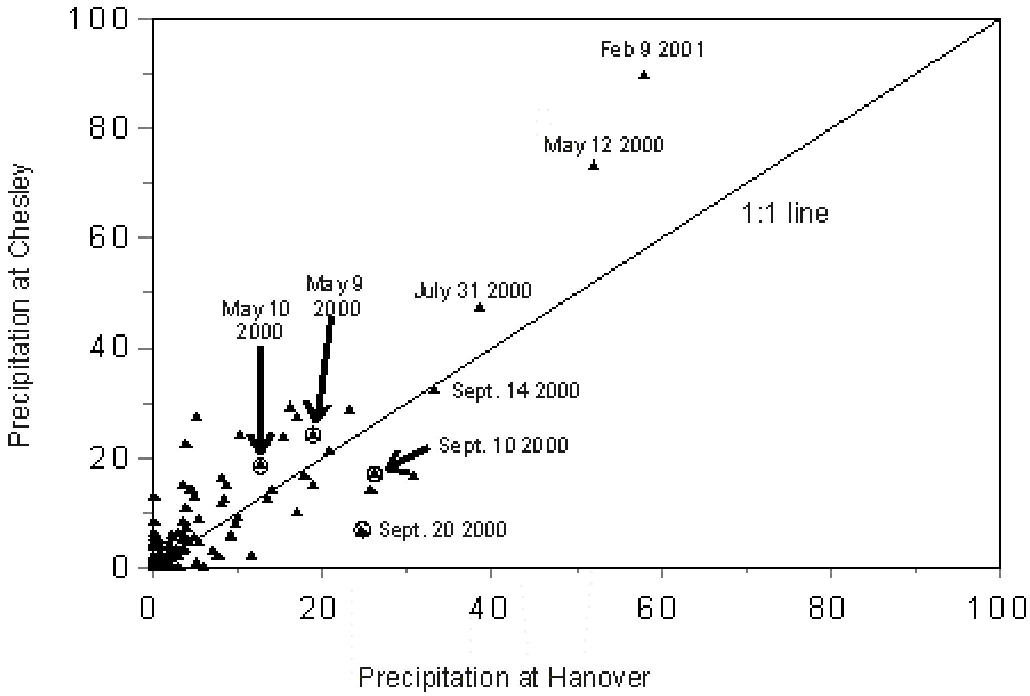

Figure 19 Correlation between daily precipitation values at Hanover and at Chesley over the period data May 1 2000 to April 17 2001, showing that there are often substantial differences between the two locations (data from Saugeen Valley Conservation Authority).

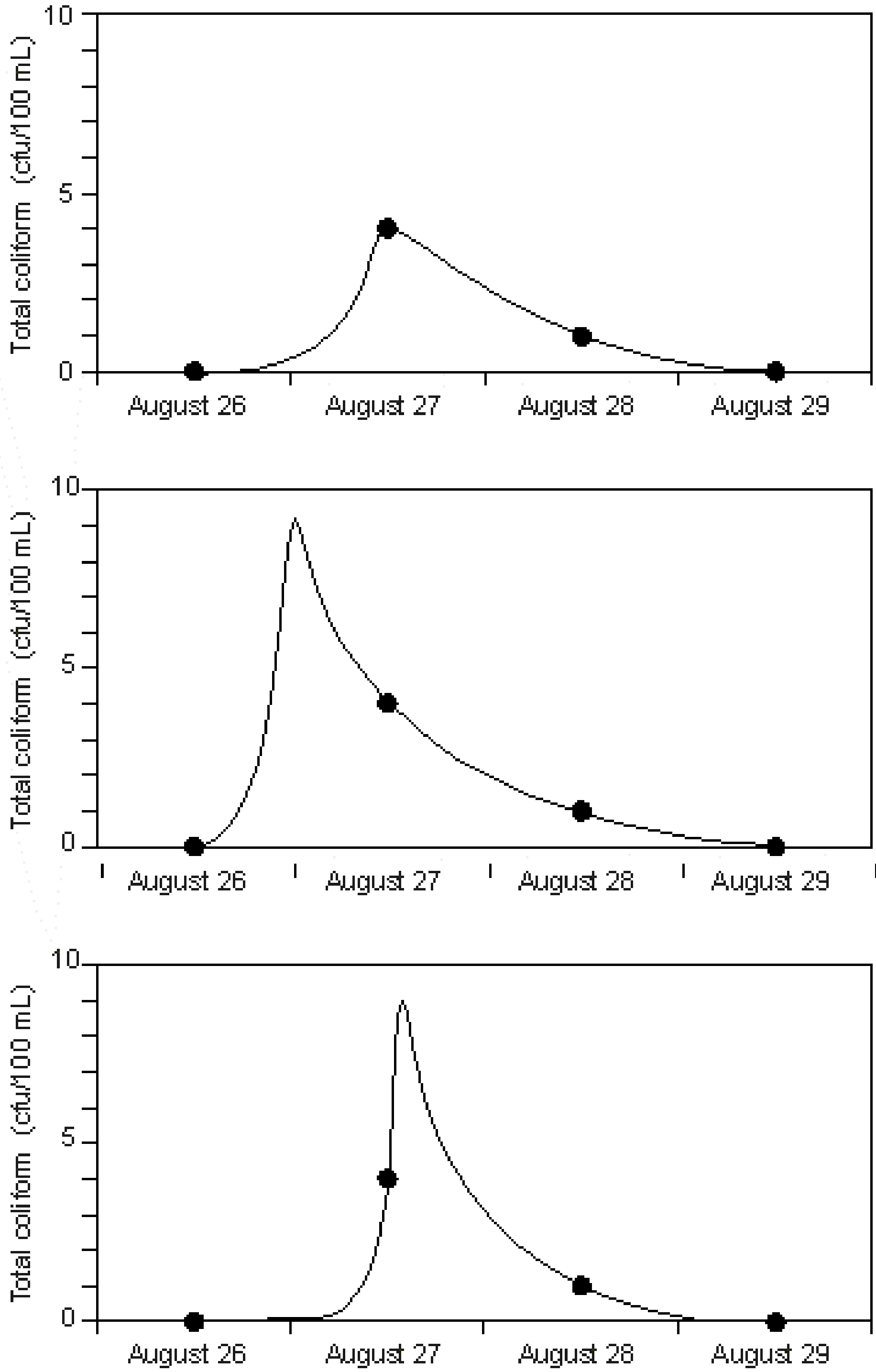

Figure 20 Three possible interpretations of the total coliform data from Well 7 from August 26th to August 29th 2000 (data from OCWA, 2000a).

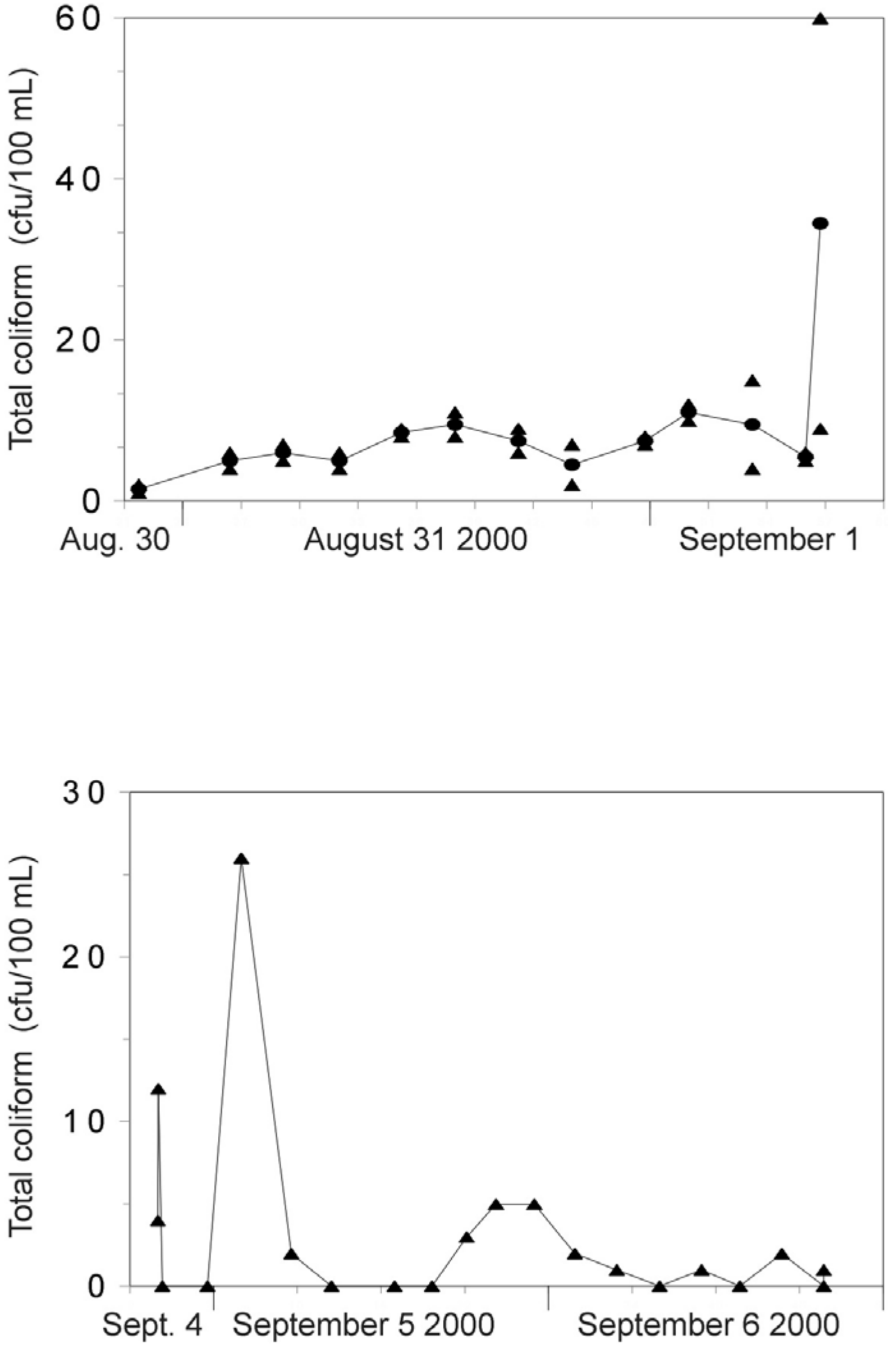

Figure 21 Variation in total coliform during the pumping test at Well 5 (top) and at Well 6 (bottom). The individual results at Well 5 are shown by triangles, and the solid line and circles represent averages of two samples taken at the same time (data from Golder Associates, 2000b, Tables 8 and 14).

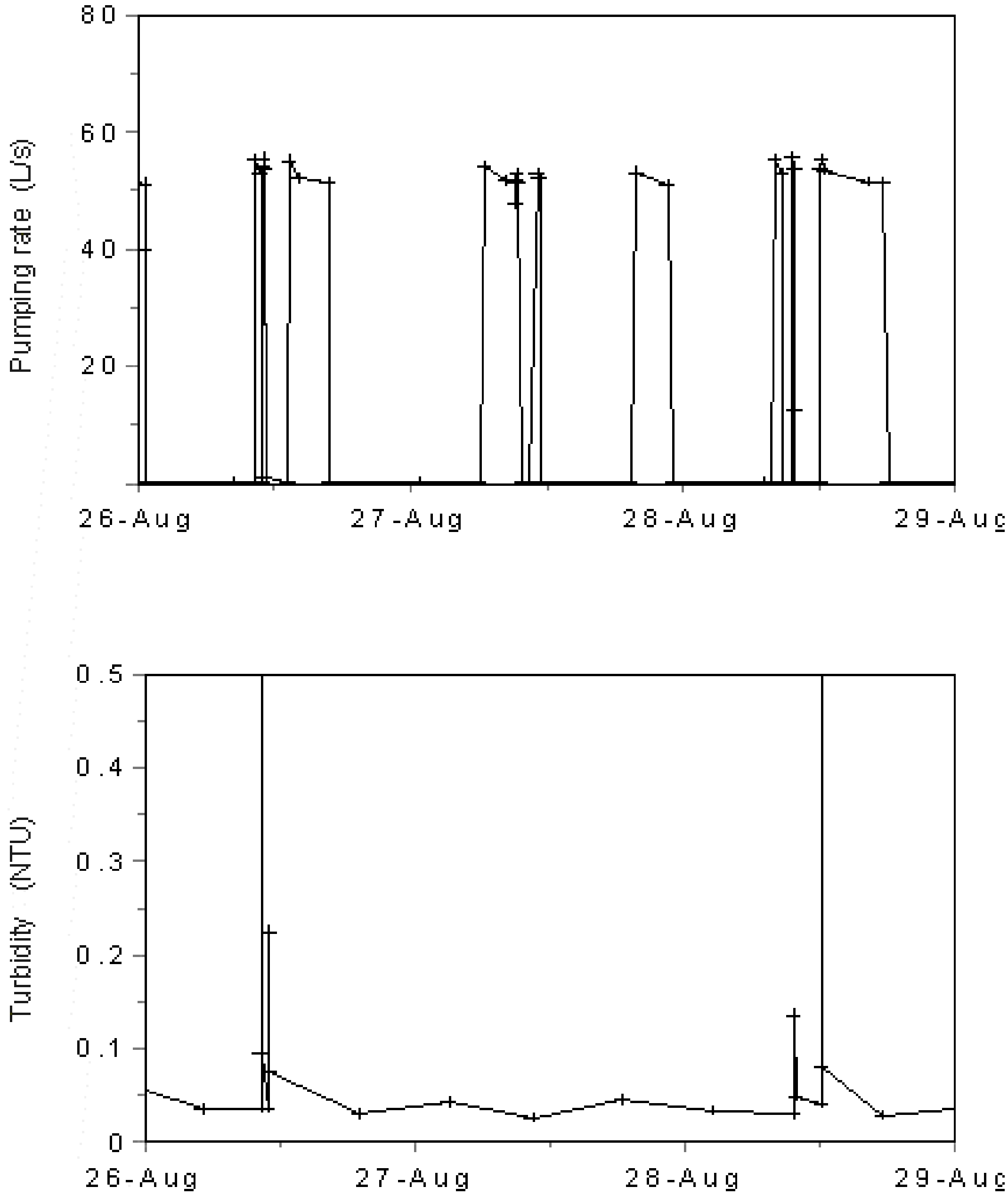

Figure 22 Pumped discharge (top) and turbidity (bottom) at Well 7 during the period August 26th 2000 to August 28th 2000 at a time that there was bacterial contamination of the well. From SCADA records, courtesy of OCWA.

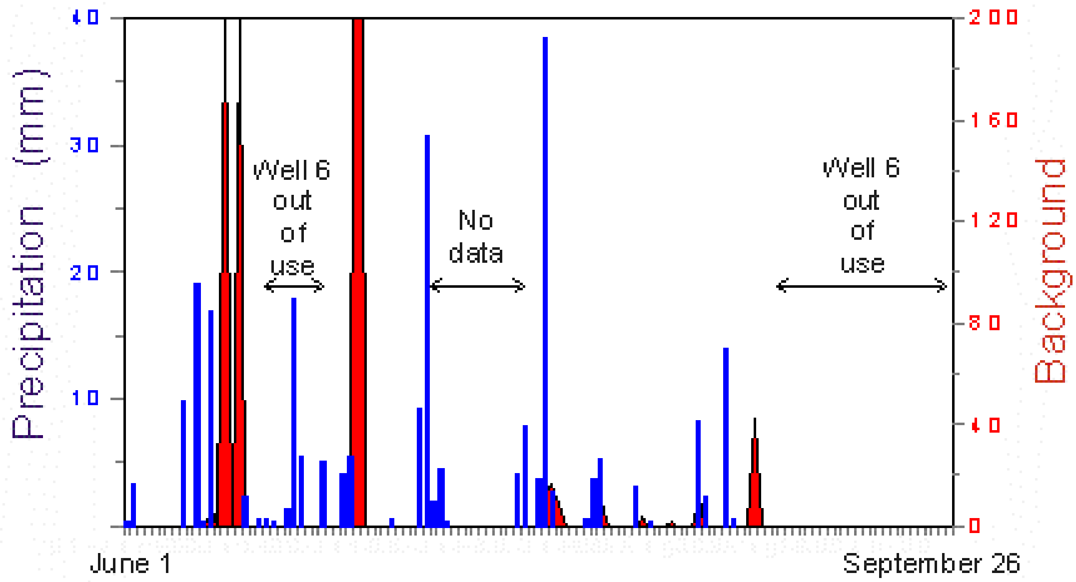

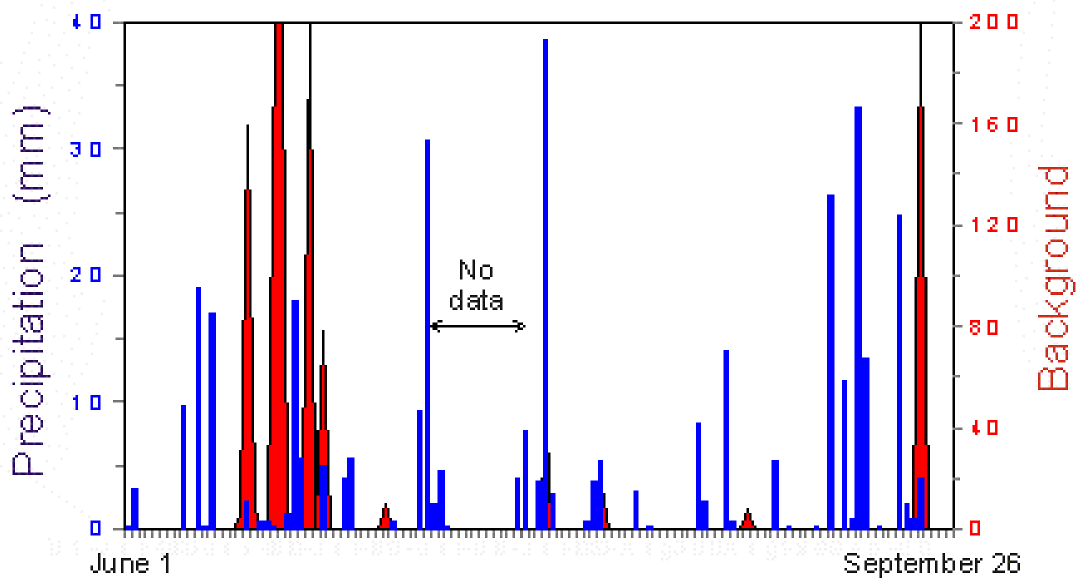

Figure 23 Background bacteria in the raw water at Well 6 (top) and at Well 7 (bottom) from June 1 to September 26 together with precipitation. Dat from OCWA (2001a and 2001b).

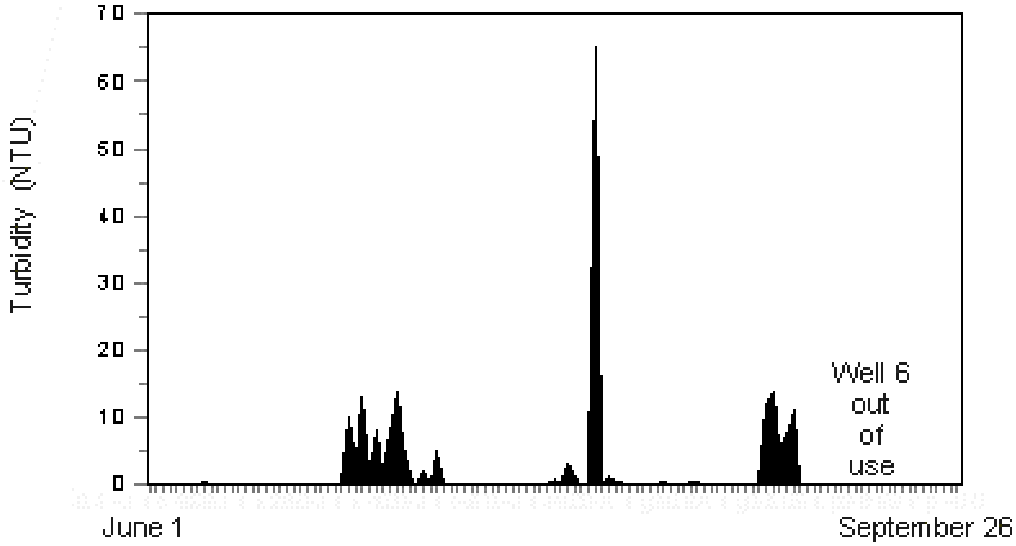

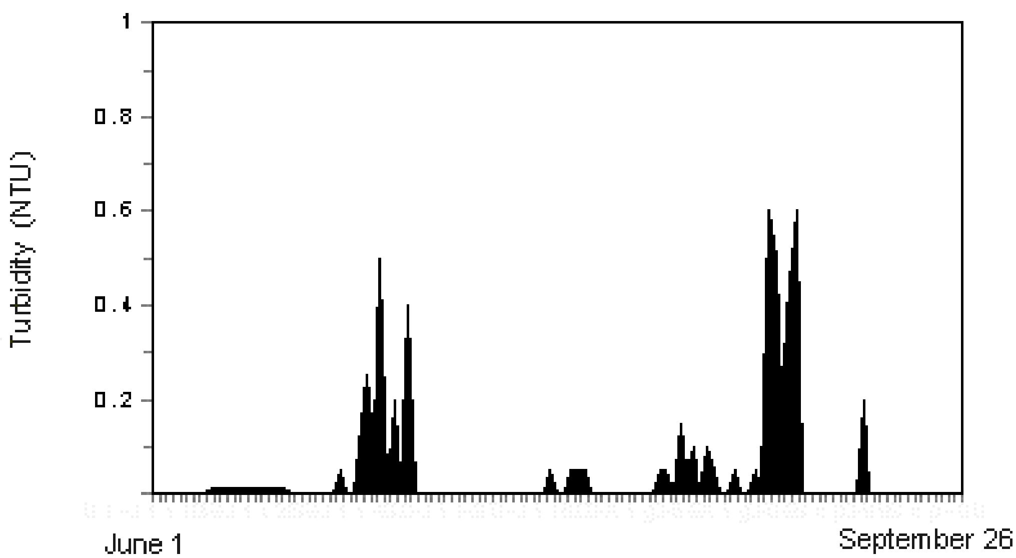

Figure 24 Turbidity in the raw water at Well 6 from June 1 to August 31 2000 (top) and at Well 7 from June 1 to September 26 2000 (bottom). Data from OCWA (2000a and 2000b).

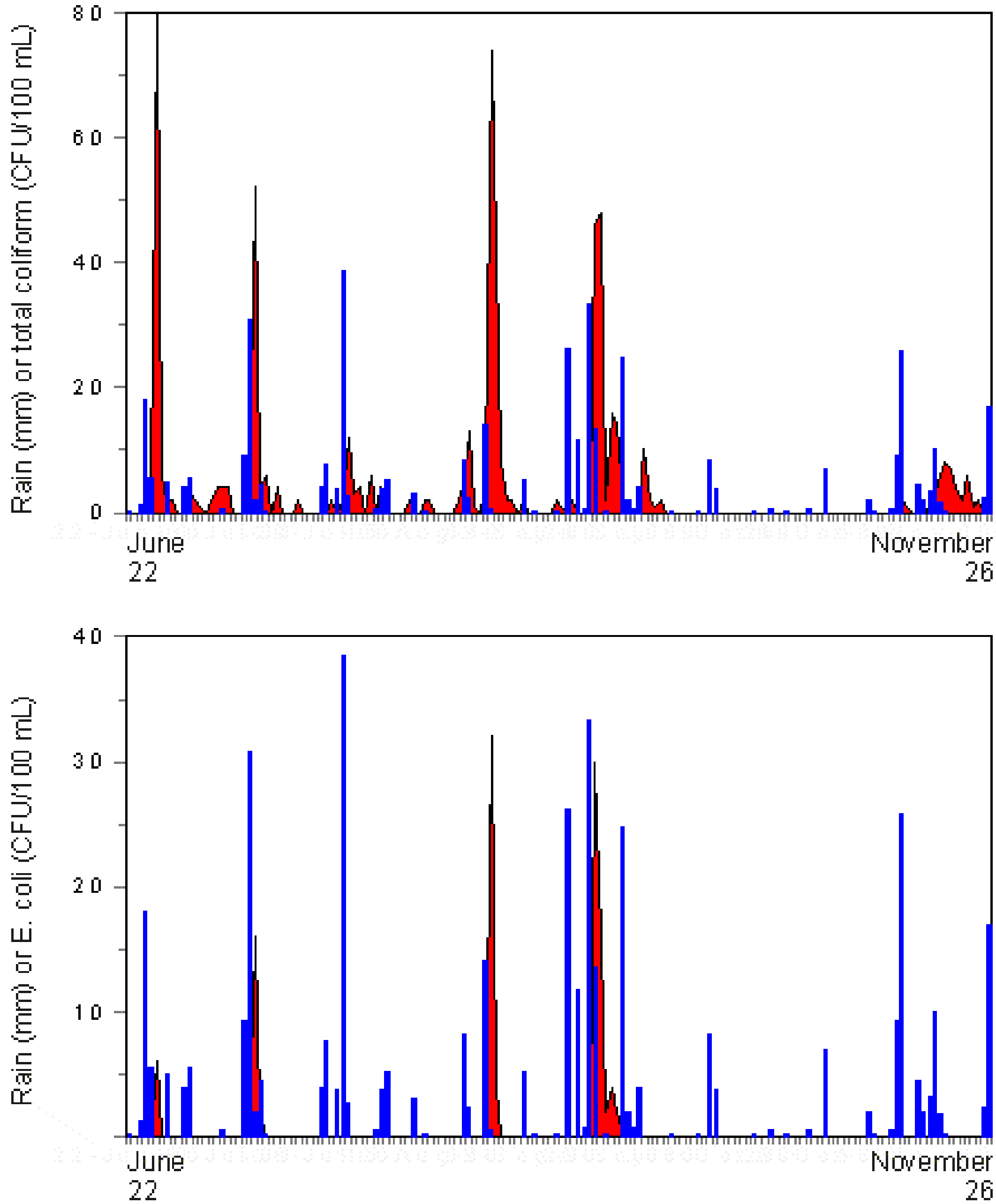

Figure 25 Correlation between total coliform (top) or E. coli (bottom) at a domestic well west of Walkerton and precipitation at the Saugeen Valley Conservation Authority gauge between Hanover and Walkerton (bacteria data from Goss, 2001b).

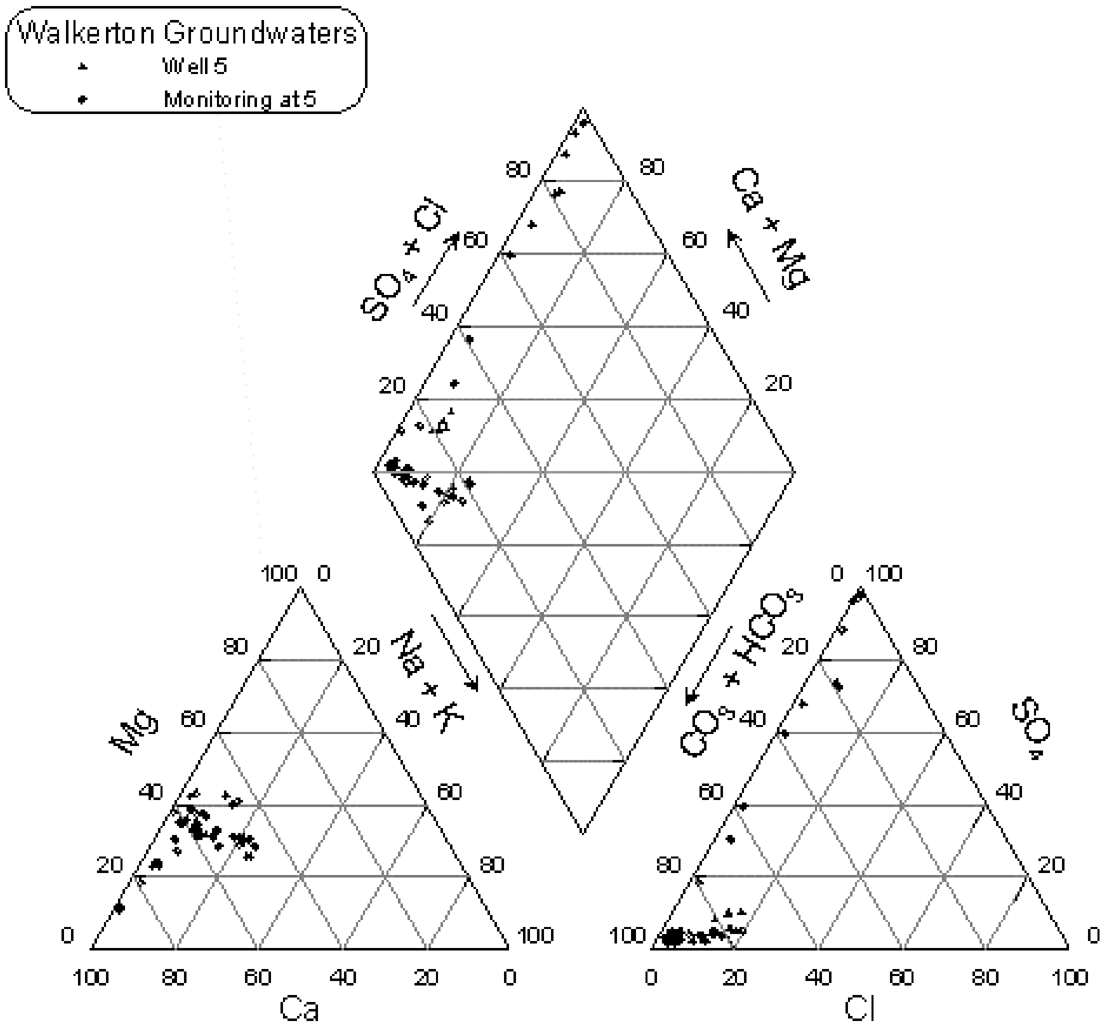

Figure 26 Piper diagram showing the major ions in the groundwater at Well 5 and at the nearby monitoring wells (data from Golder Associates, 2000a and 2000b).

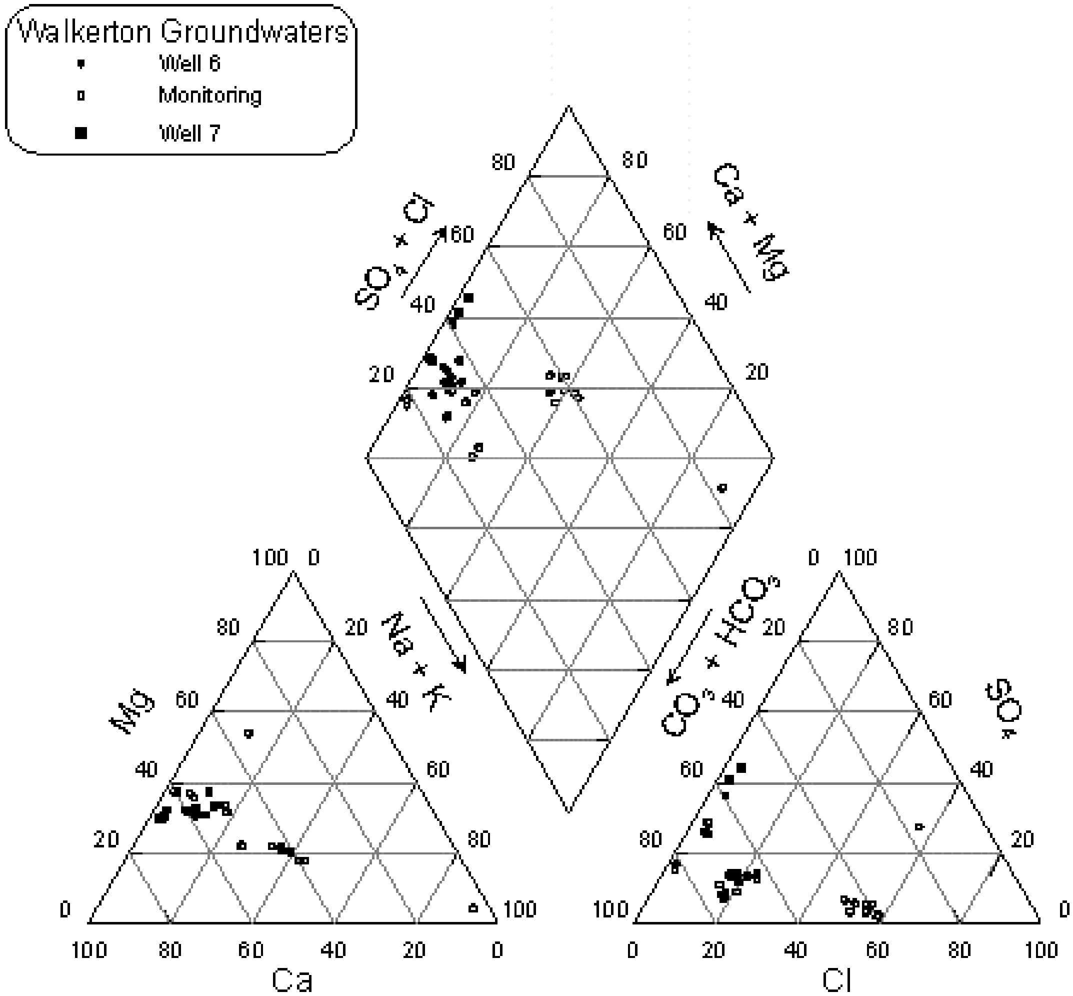

Figure 27 Piper diagram showing the major ions in the groundwater at Wells 6 and 7 and at the nearby monitoring wells (data from Golder Associates, 2000a, b).

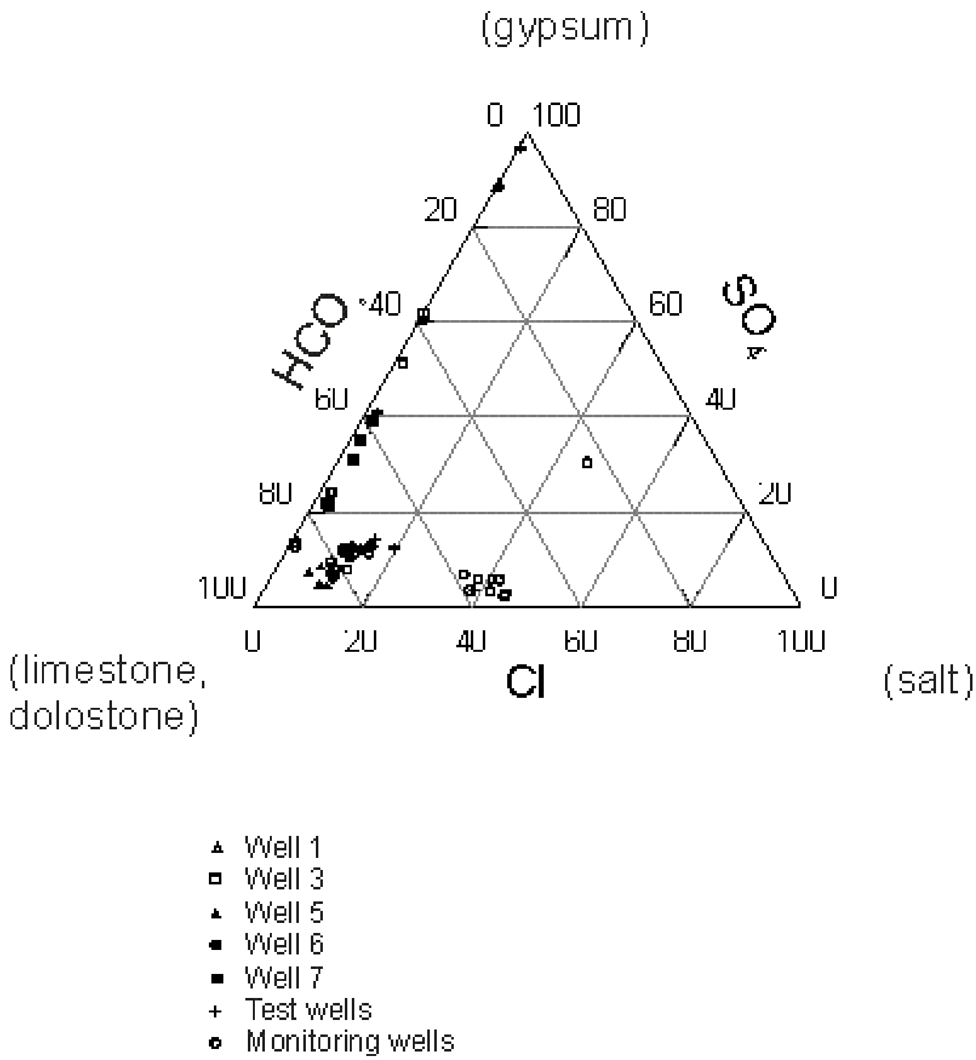

Figure 28 Plot of anions for water samples from Walkerton, showing the rocks from which the anions are commonly derived in the Walkerton area (data from Golder Associates, 2000a and 2000b).

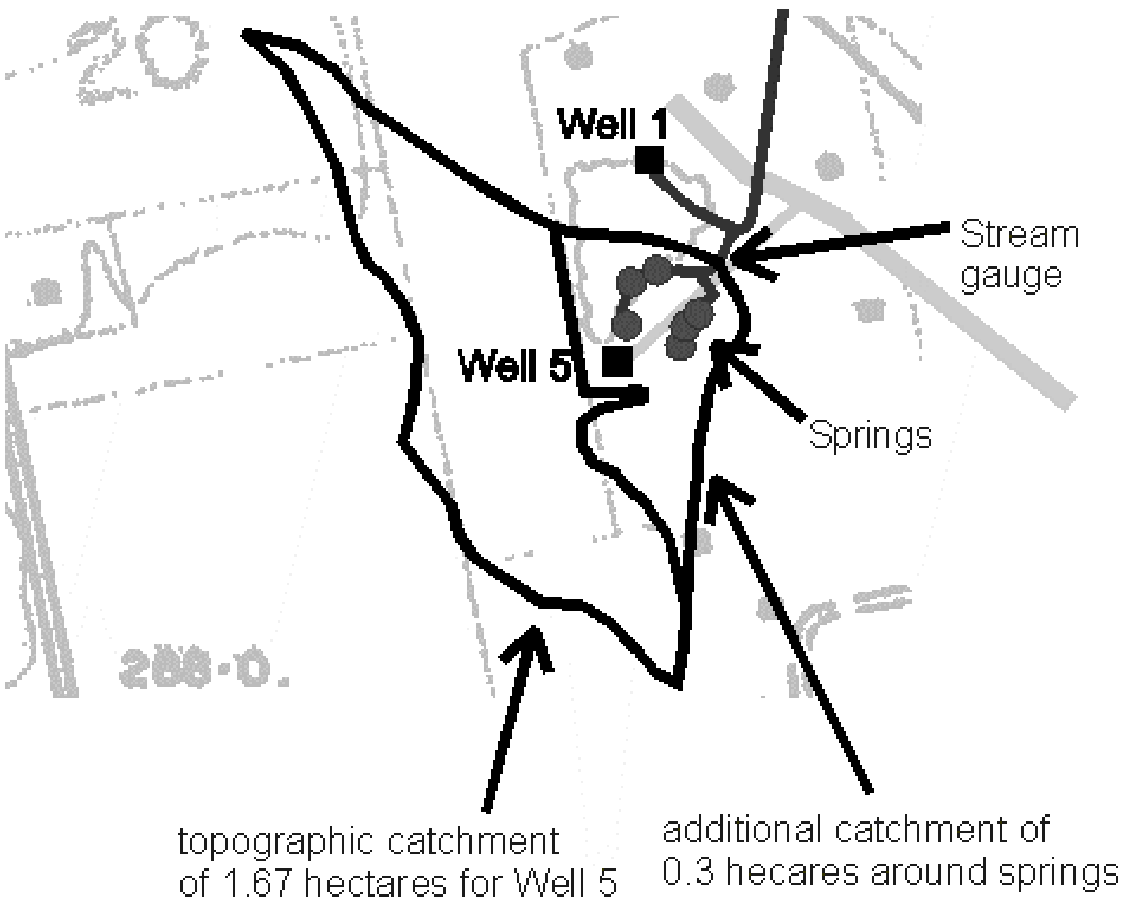

Figure 29 Location of the springs close to Well 5 and the surface catchment area of 2.0 hectares for the springs (in part after B.M. Ross and Associates, Exhibit 221, Appendix L)

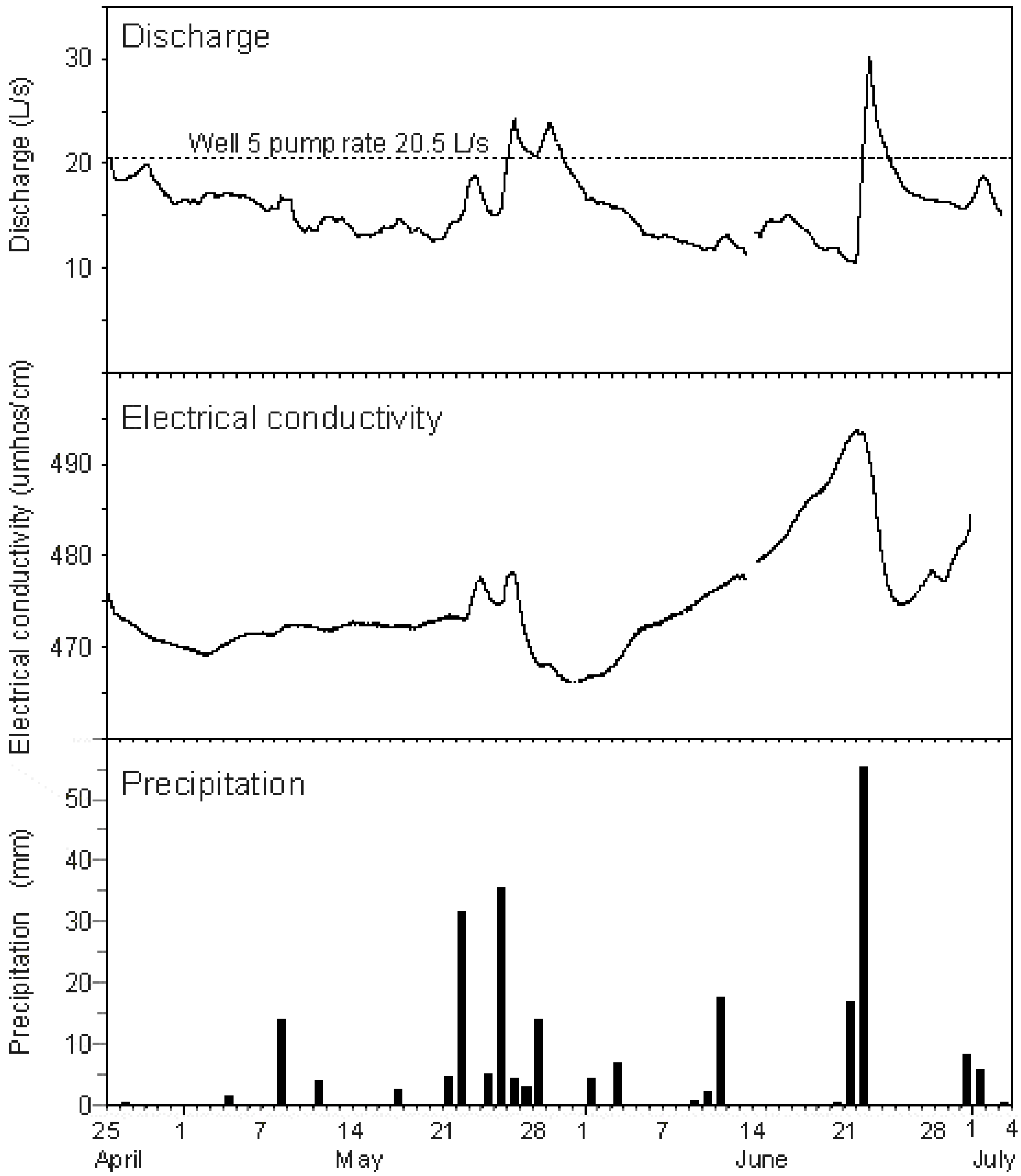

Figure 30 Discharge and electrical conductivity of the Well 5 springs, and precipitation at Well 7

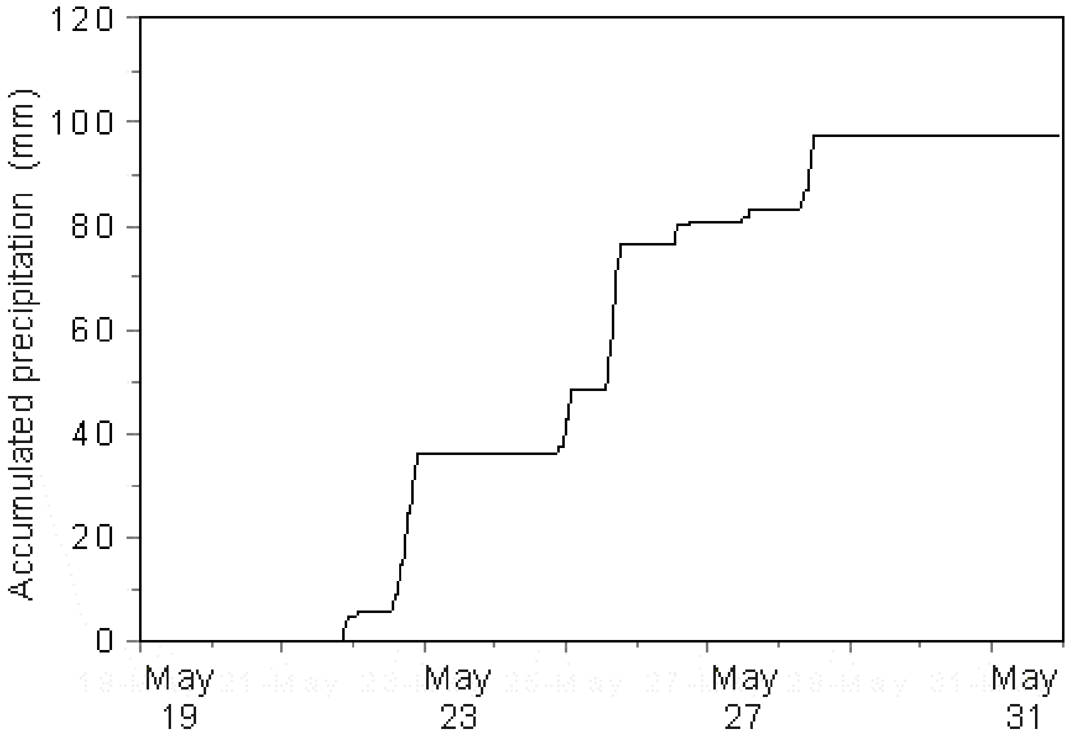

Figure 31 Accumulated precipitation at a rain gauge beside Well 7, showing major rain events on May 22nd, 25th, and 28th 2001

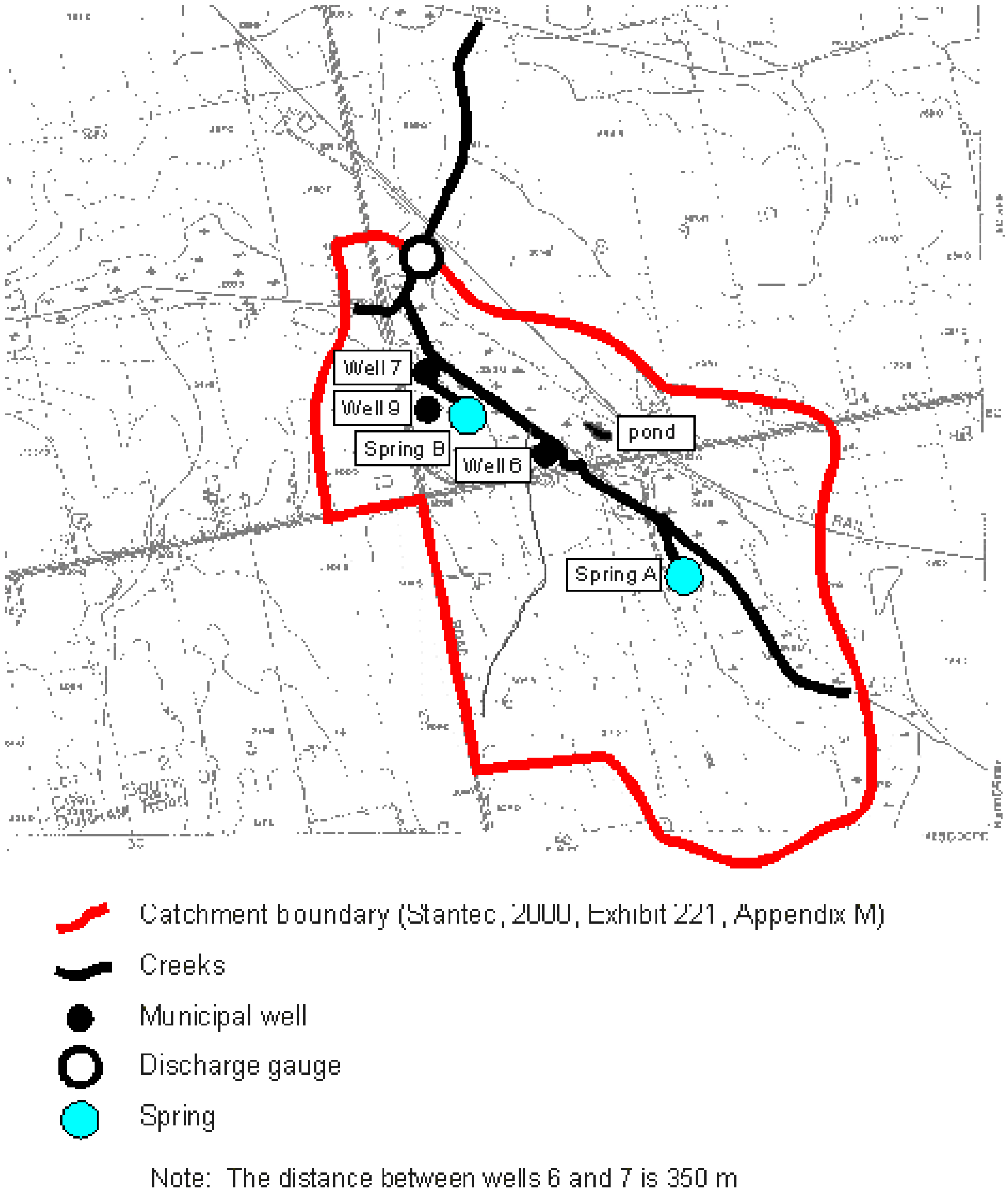

Figure 32 Location of the springs close to Wells 6, 7 and 9 and the boundary of the 117 hectare (0.45 square mile) surface catchment surrounding the wells

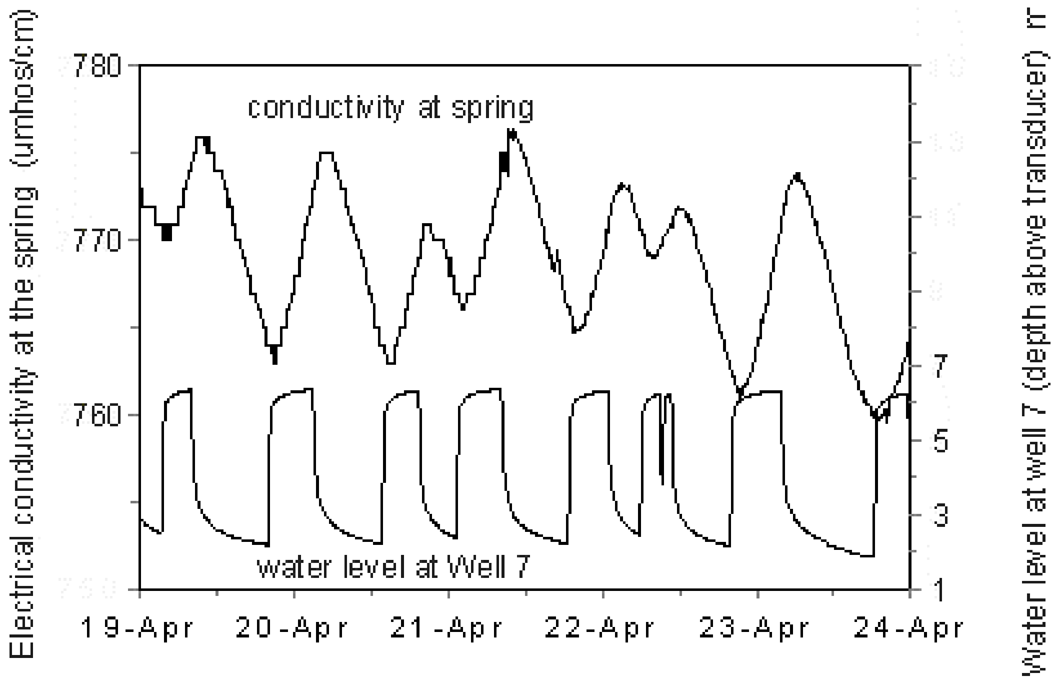

Figure 33 Correlation in the variation in electrical conductivity at the spring between Wells 6 and 7 with pumping at Well 7

Test Well 1-86 Pump

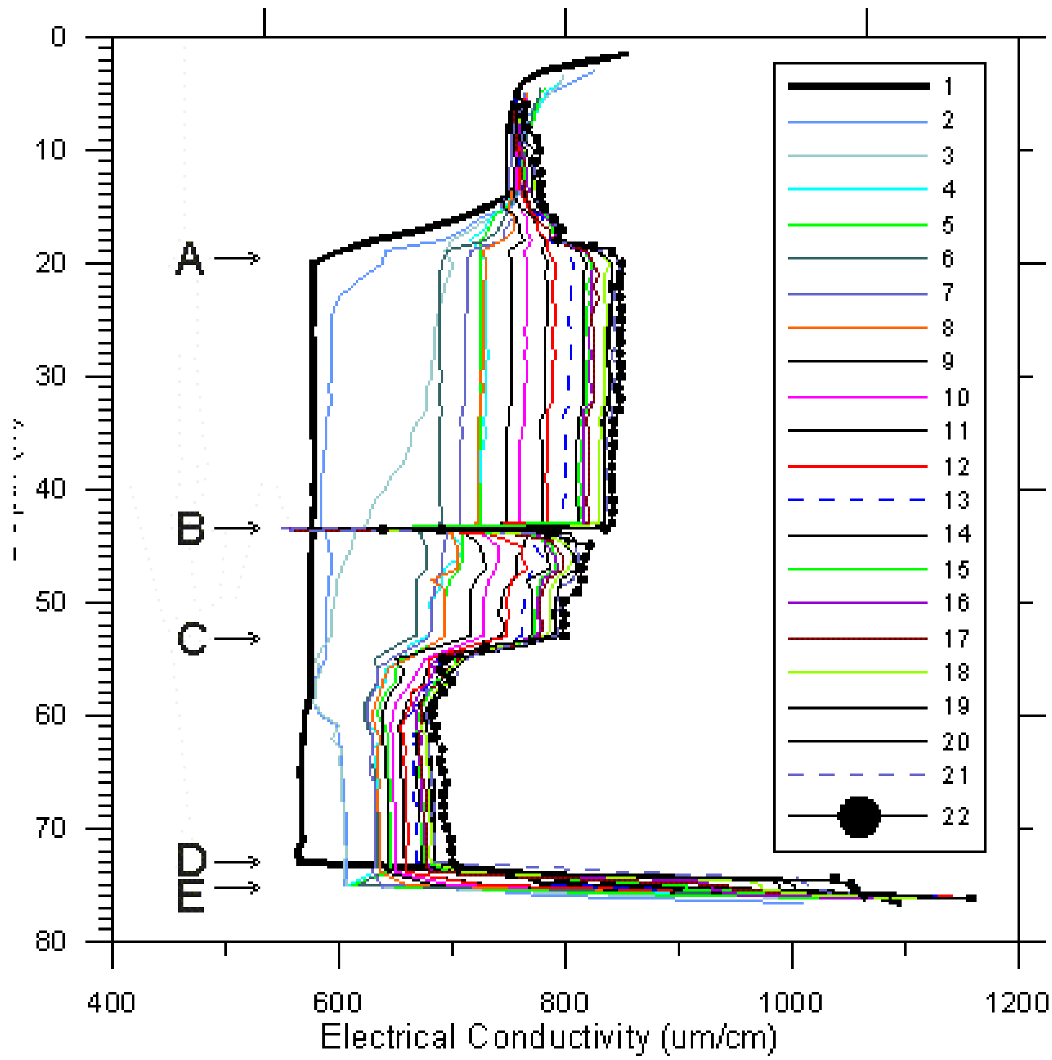

Figure 34 Sequential profiles of electrical conductivity during the 72 hour pump test at Well 9 on June 10-14 2001

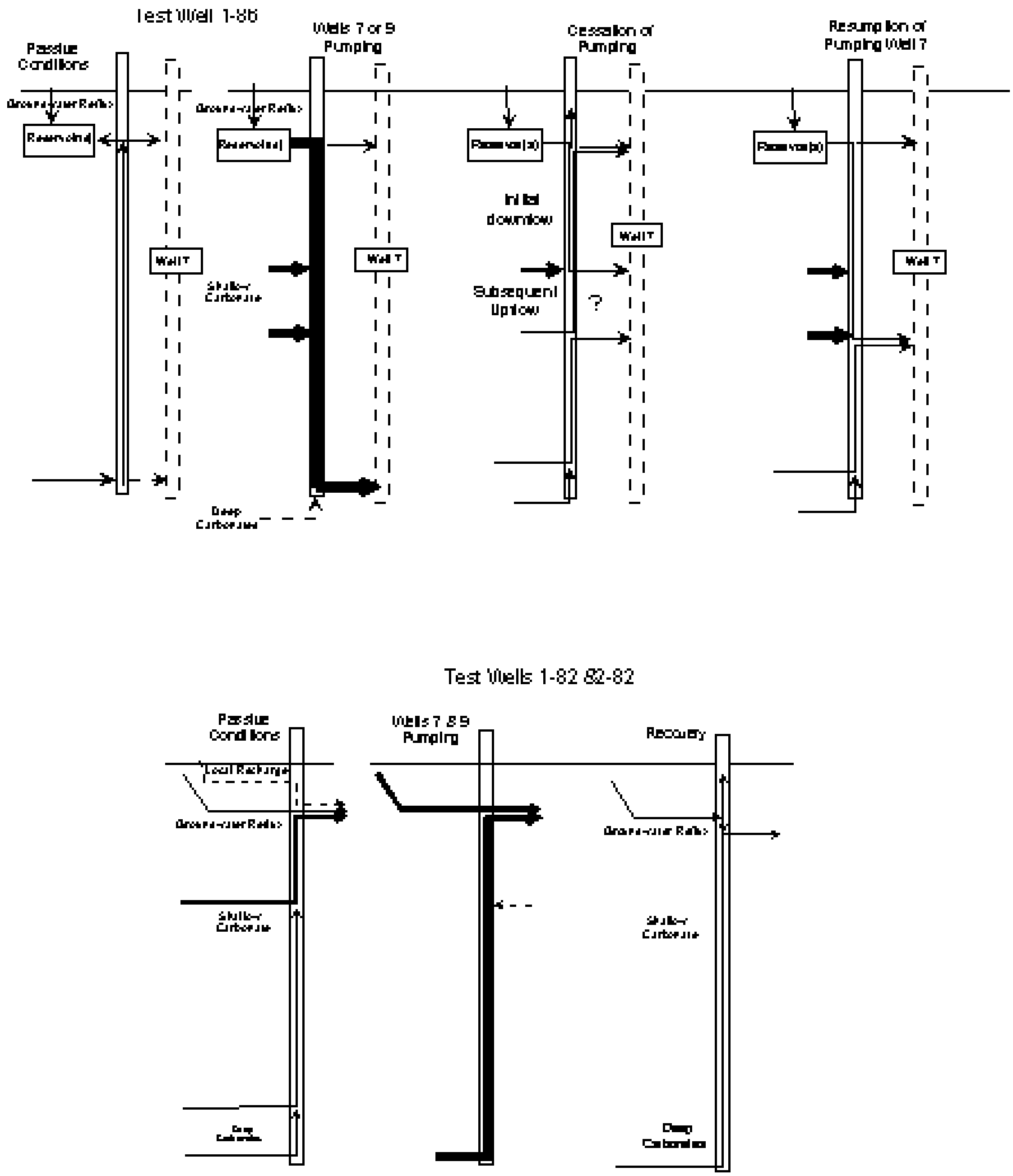

Figure 35 Summary of flow patterns in TW1-86 (top) and in TW1-82 and TW2-82 (bottom) during pumping and non-pumping conditions

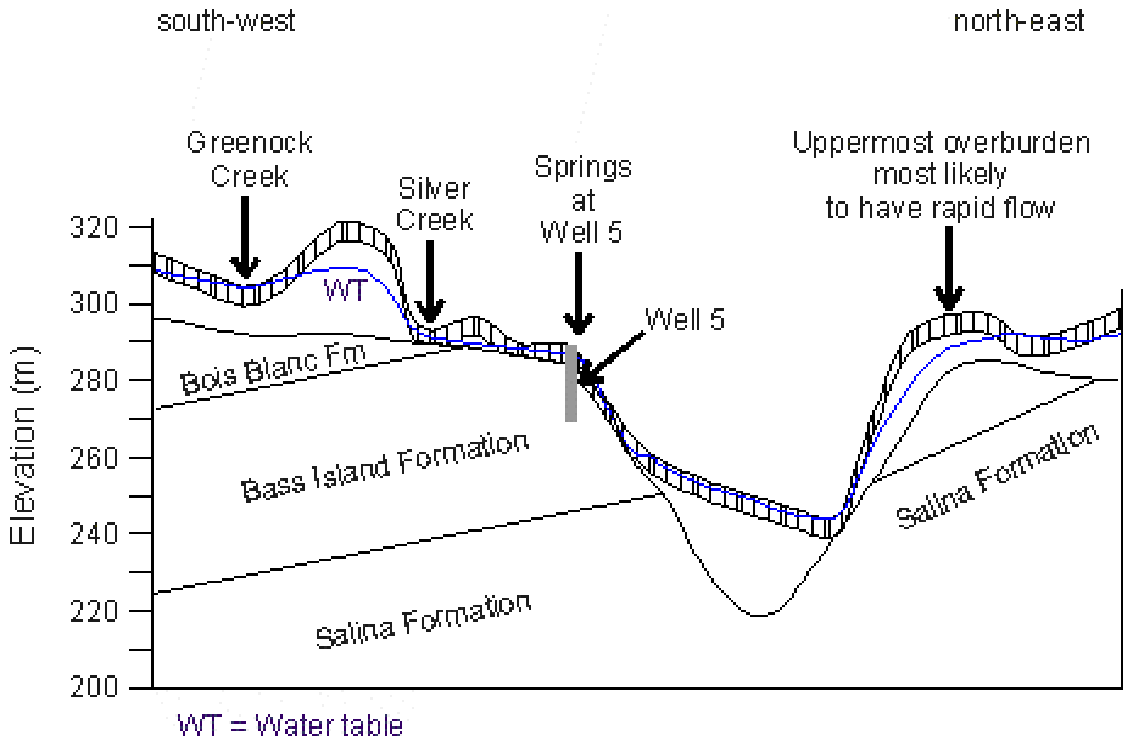

Figure 36 Geological cross-section through Well 5 (geology after Liberty and Bolton, 1971). Note that there is considerable vertical exaggeration in the diagram.

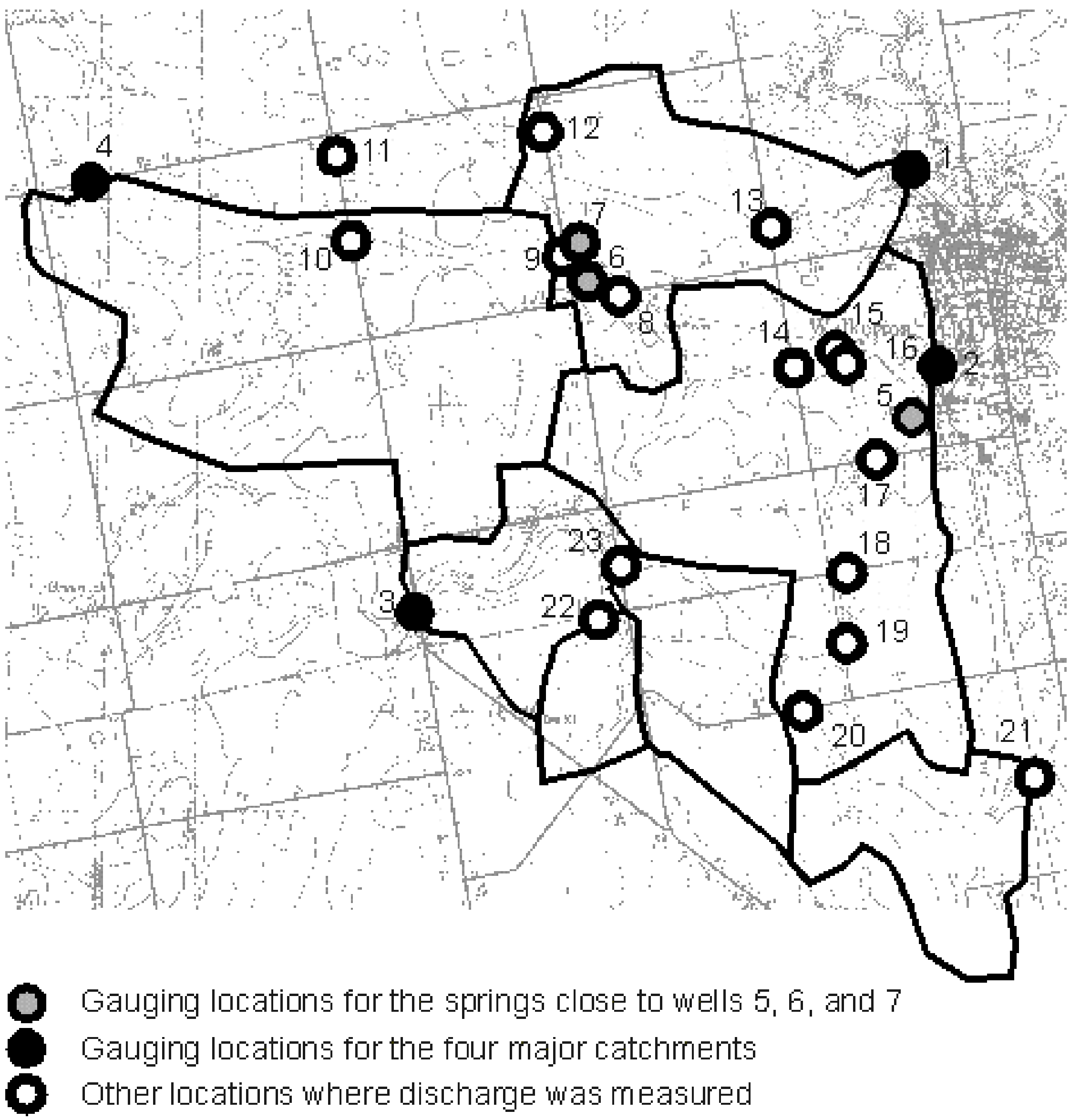

Figure 37 Locations where discharge was measured

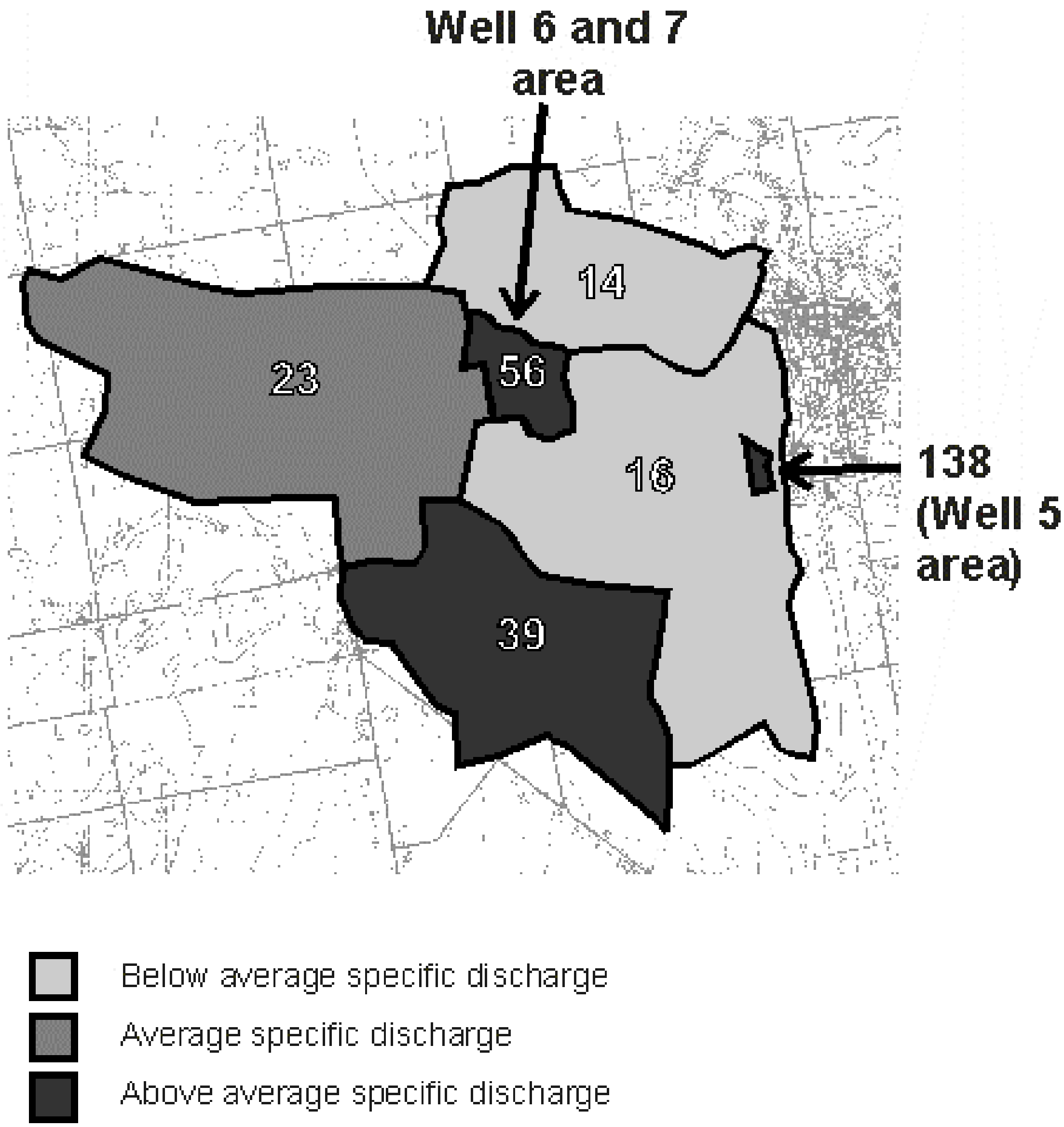

Figure 38 Specific discharge (in litres per second per square kilometre) for the areas around Wells 5, 6, and 7, showing anomalously high specific discharge for the spring areas

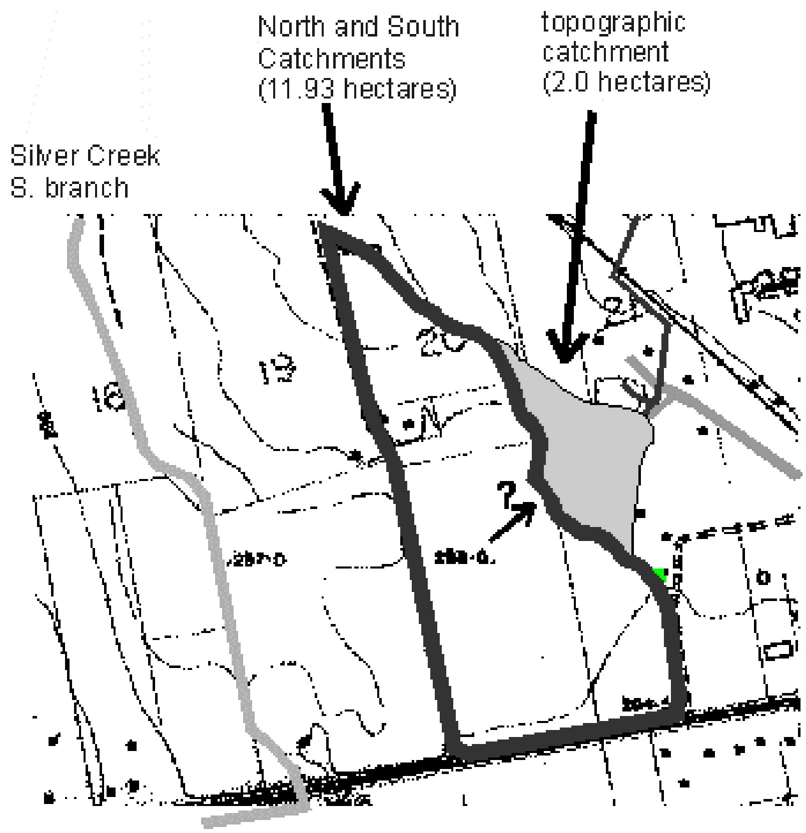

Figure 39 Topographic catchment of 2.0 hectares (shaded) and the possible additional 11.93 hectare catchment that could also possible contribute overland flow to the Well 5 area following intense rain (after B.M. Ross, Exhibit 221, Appendix L)

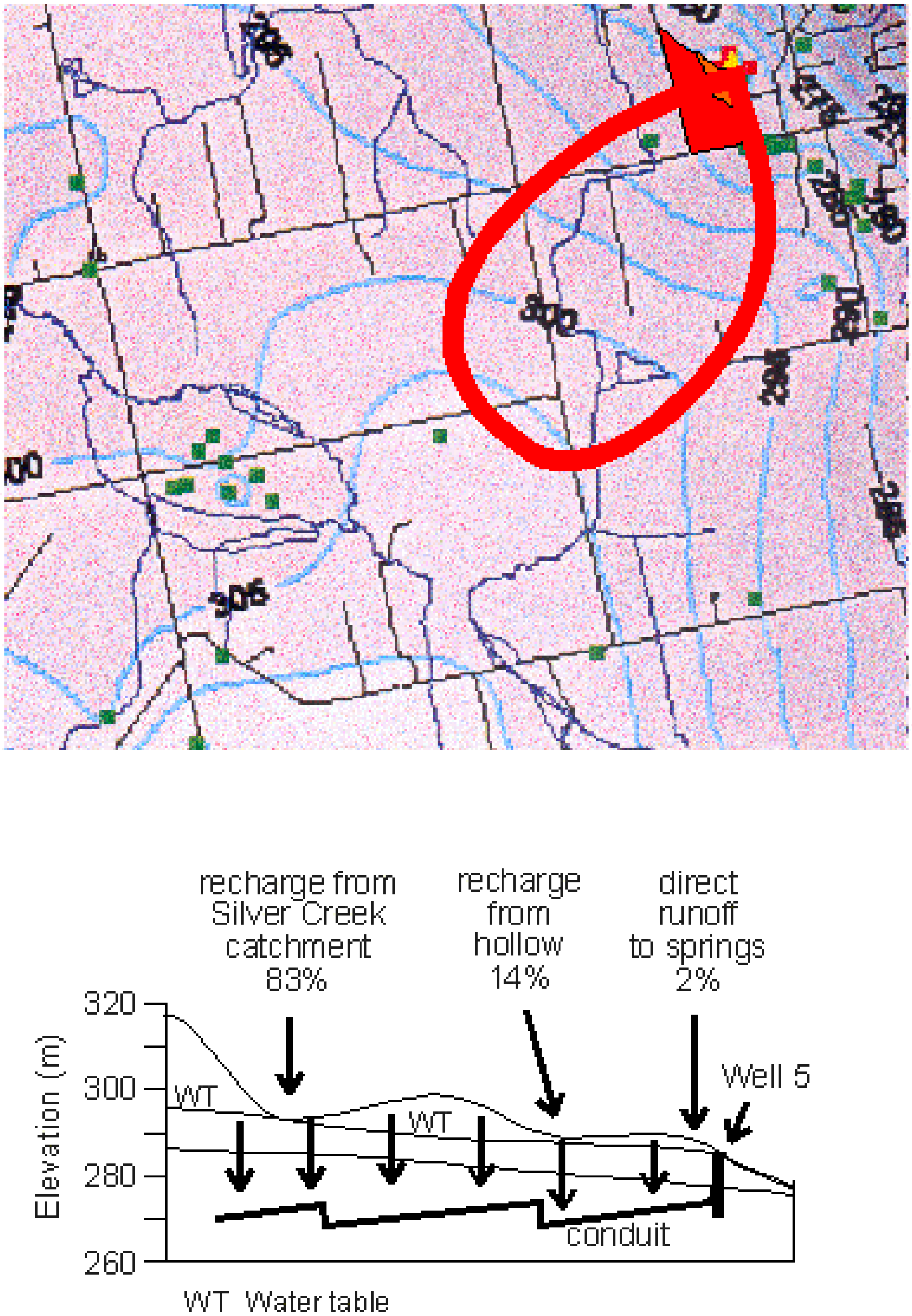

Figure 40 Plan of the approximate groundwater catchment for the springs at Well 5, superimposed on the water level map based on MOE records (from Golder Associates, 2000a, Figure 12) (top) and profile through the catchment area for the springs (bottom)

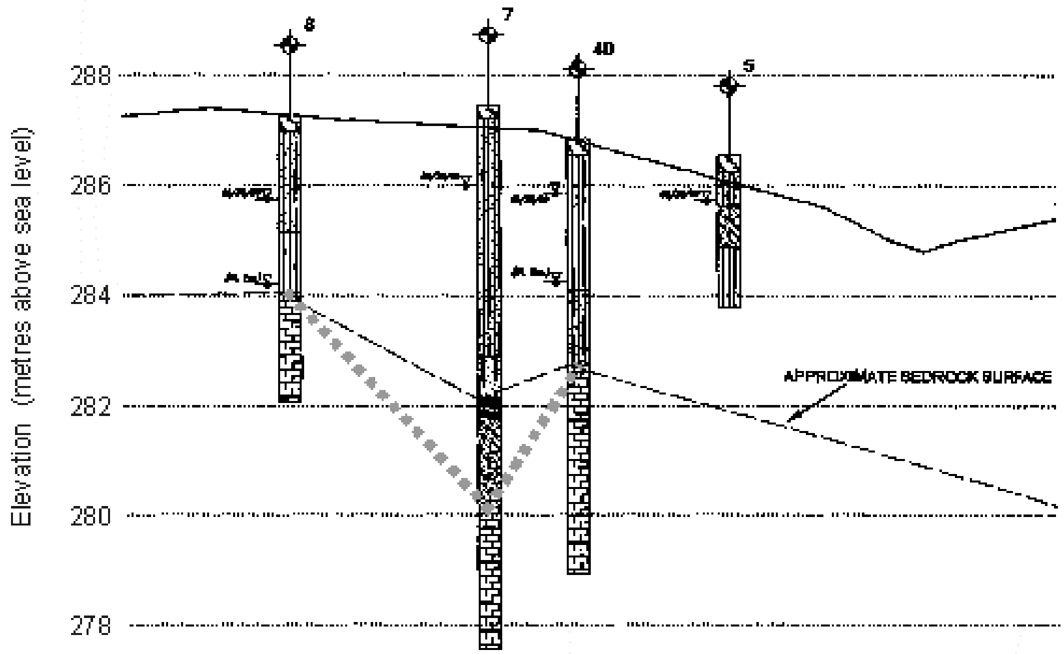

Figure 41 Bedrock surface close to Well 5 (from Golder report, September 2000, Exhibit 259, Figure 11). At monitoring well 7 there are two possibilities:

a) bedrock surface at 282.13. In this case there is 1.68 m high cave below 31 cm of bedrock

b) bedrock surface at 280.14 m. In this case a 13 cm thick boulder was drilled through.

Notes: monitoring well 5 is adjacent to Well 5
the vertical exaggeration is times 10

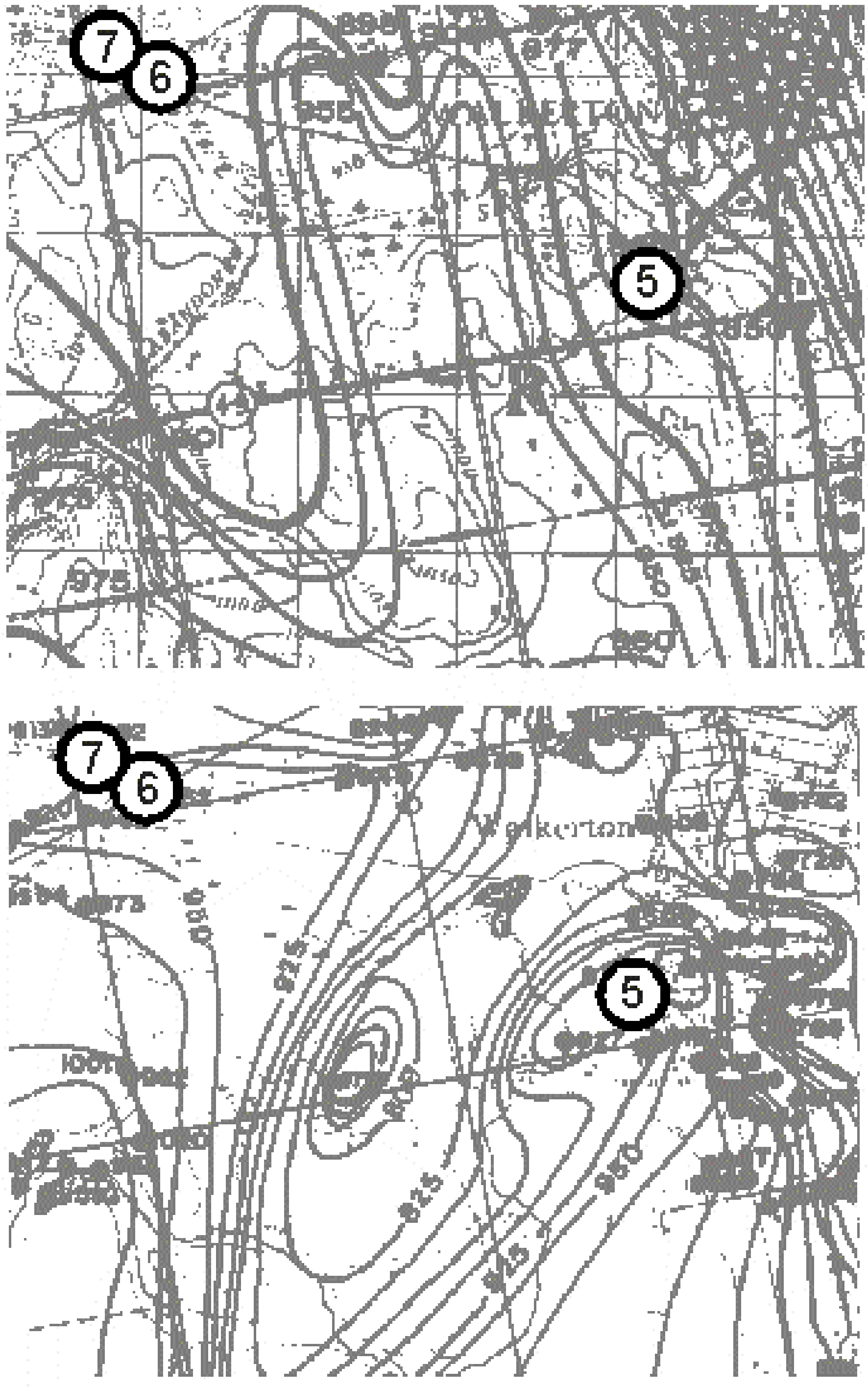

Figure 42 Bedrock topography in the areas of Wells 5, 6, and 7 from provincial 1:50,000 maps P165 (Davis and McClymont, 1962; top) and P3207 (Kelly and Carter, 1993; bottom). Wells 5, 6, and 7 are indicated on the map. Both maps have a 25 foot contour interval.

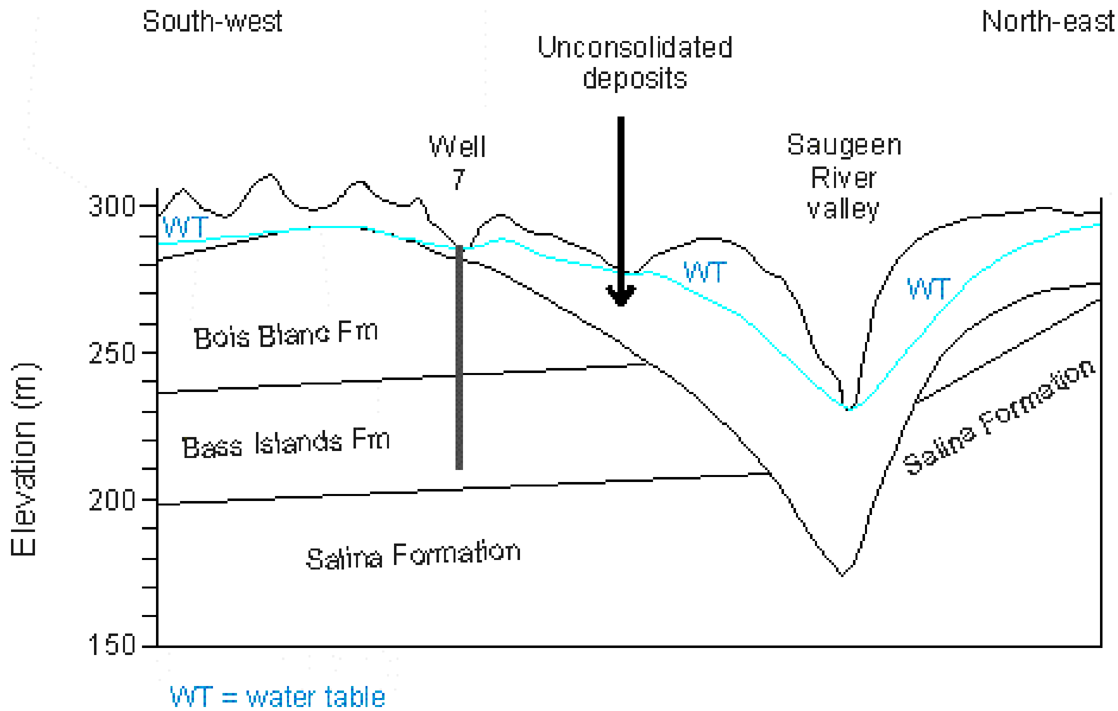

Figure 43 Geological cross-section through Well 7 (geology after Liberty and Bolton, 1971). Note that there is considerable vertical exaggeration in the diagram.

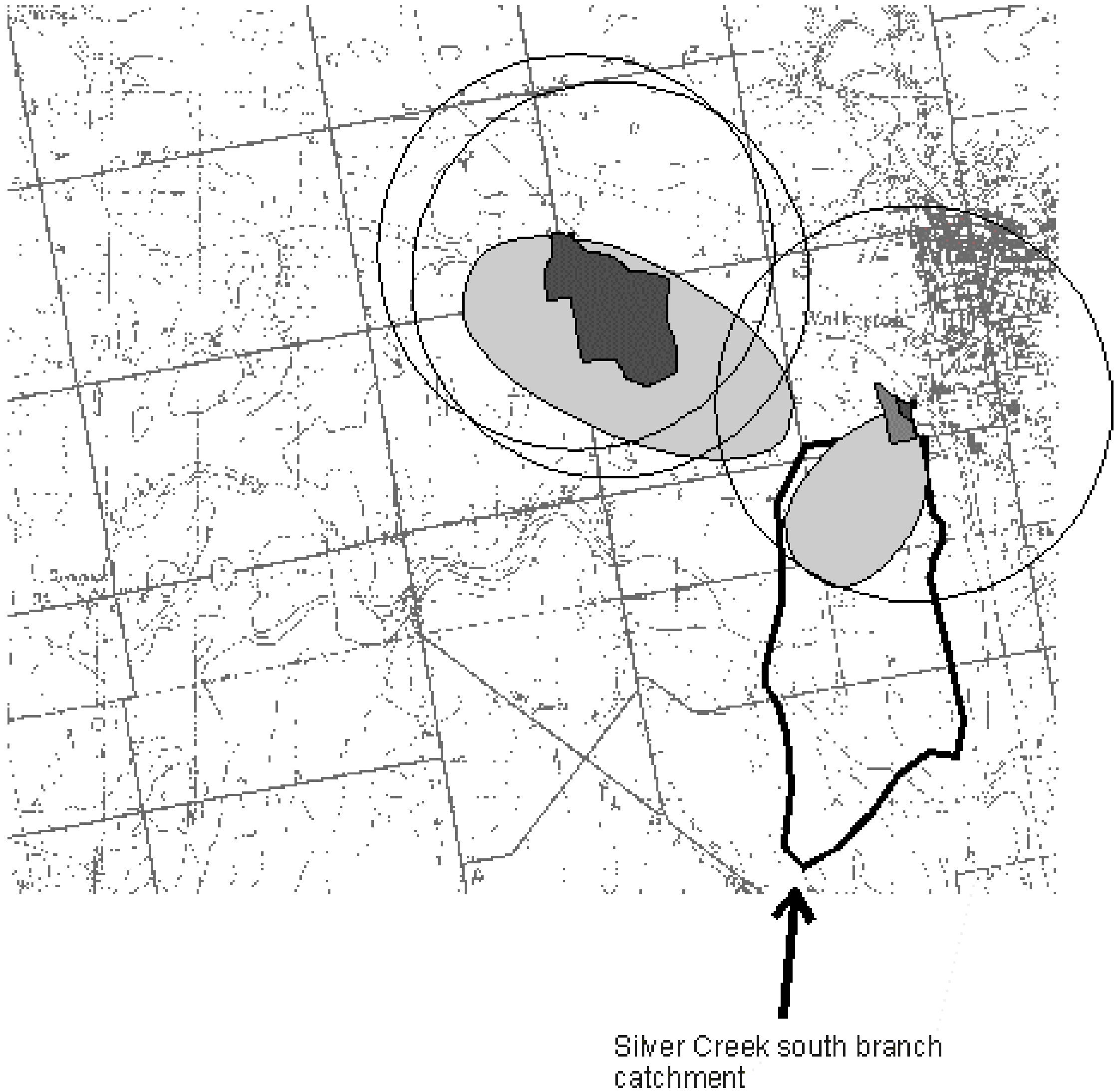

Figure 44 Approximate catchment zones for Wells 5 and for 6/7. The surface catchment zones for the spring areas are shown in dark grey and the groundwater catchments are shown in light grey. The possible extension of the surface catchment zone for the Well 5 area which might flow to Well 5 after heavy rain is shown in medium grey. The three circles each have a radius of 4 km around Wells 5, 6, and 7, respectively, which represents the radius within which there was environmental testing of livestock farms (Bruce-Grey-Owen Sound Health Unit, 2000, p. iii).

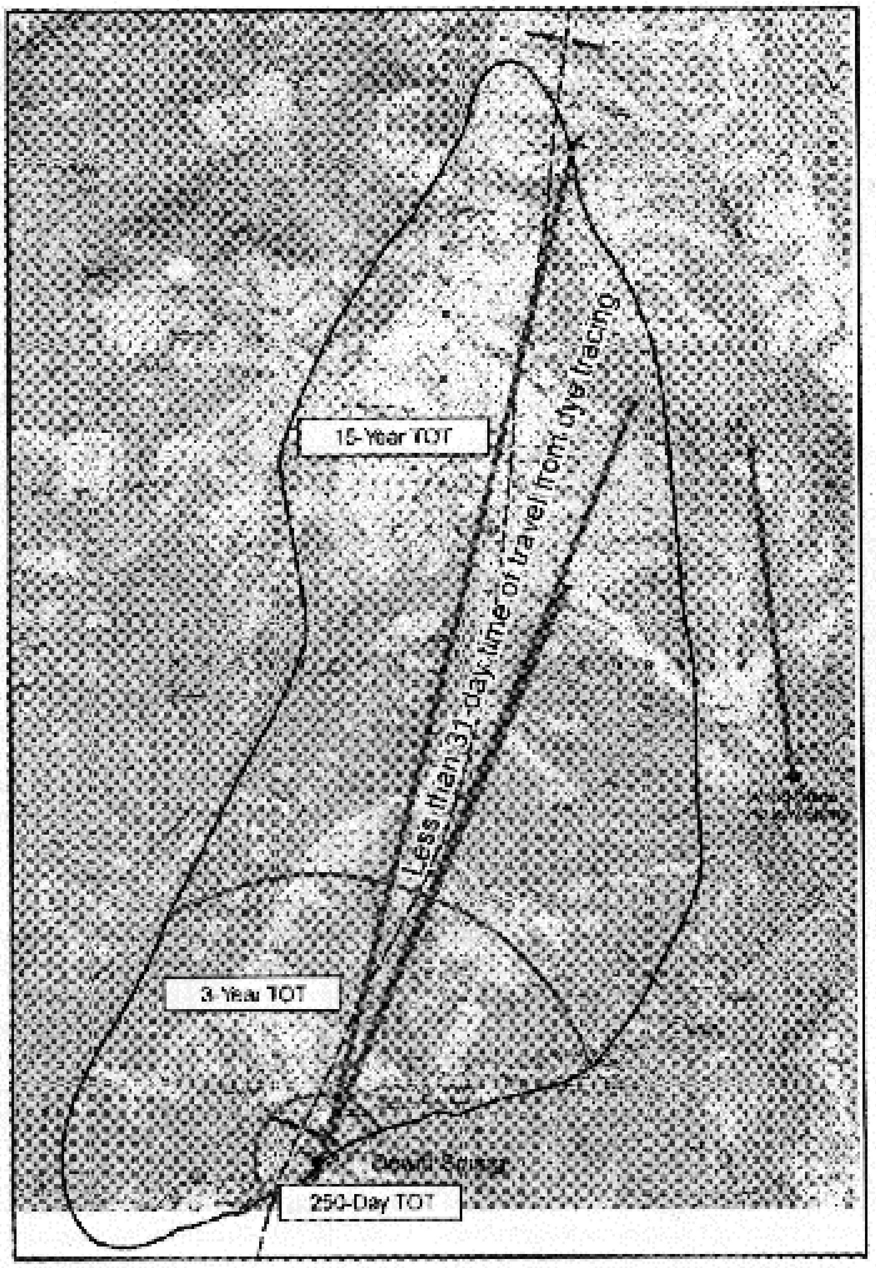

Figure 45 Time of travel (TOT) zones for groundwater flow to Dewitt Spring, Utah, based on the assumption that the carbonate aquifer behaves as a porous medium, and the trajectories of three subsequent tracer tests which all took less than 31 days to travel 6.9 to 11.6 km to the spring (from Spangler, 1999; see Appendix 3)